Interactive comment on "Comparison of Different Sequential Assimilation Algorithms for Satellite-derived Leaf Area Index Using the Data Assimilation Research Testbed (lanai)" by Xiao-Lu Ling et al.

Anonymous Referee #1

Received and published: 25 February 2019

Major comments

The submitted paper uses four assimilation methods (KF, EnKF, EAKF and PF) and CLM4CN to assimilate LAI, and chooses a best assimilation method by comparing with MODIS LAI. MODIS satellite remote sensing data can obtain LAI products with long time series. However, due to the impacts of cloud cover, aerosols, snow cover, and sensor failure, MODIS LAI products are characterized by high noise, low accuracy, and large fluctuations in the time series. Therefore, MODIS LAI data with better quality should be selected as observations based on quality control (QC) information. The research objective is reasonable and the review portion and figures need to be improved.

Response: We appreciate your comments, which are helpful for us to further improve this paper. In the revised manuscript, we have focused on the following issues.

1. Proofreading has been done to improve the readability and quality of this manuscript. The quality of all the figures has also been improved.
2. The description for the experimental design and spin-up process has been added to Section 2. The ensemble simulation during the time period of 1998 ~ 2001 is treated as spin-up, which explains why the result is shown for the year 2002.
3. The datasets for assimilation and estimation are introduced in Section 2.4.2. The Global Land Surface Satellite (GLASS) LAI dataset is used as observations for assimilation. To evaluate the assimilation result, an improved LAI dataset developed from the MODerate Resolution Imaging Spectroradiometer (MODIS) is utilized, which can reduce the spatial and temporal inconsistencies by considering the characteristics of the MODIS LAI data and quality control (QC) information

Specific comments

1. What does the letter represent in formula (2)? It is not clear.

Response: If there are enough observations, the posterior density at k can be approximated by

$$p(X_k^a|Y_{1:k}) \approx \sum_{i=1}^{N} w_{i,k}\,\delta(X_k^a - X_{i,k}^a)$$

in which $\delta(*)$ is the Dirac Function and $\sum_{i=1}^{N} w_{i,k} = 1$. $p(X_k^a|Y_{1:k})$ is the posterior probability distribution, $X_{i,k}^a$ is the particle element, $w_{i,k}$ is the weight of each particle, N is the number of particles.

2. Line 13-15 in page 6, What method is used to solve the particle degradation problem in PF?

Response: We didn't do anything to solve the particle degradation problem in this study. We will address this issue in our future studies.

3. In section 2.4, time period of the atmospheric datasets is 1998-2010 in DA, why the time of LAI in the result is 2002?

Response: 80 atmospheric forcing datasets at 6-hour intervals over the period of 1998-2010 are used in this study. Considering computational cost and filter performance, only 40 members are randomly selected. The reasons why the time of LAI in the result is 2002 are given below. First, the ensemble simulation during the time period of 1998 ~ 2001 was treated as spin-up. The description of the spin-up process has been added to Section 2.4.1. Second, the purpose of this study is to find out the optimal algorithm, which needs many experiments to be conducted. Aiming at global scale and considering the computational cost, only one-year assimilation and ensemble simulation are conducted. We try to first find out the best experiment, and then conduct long-term simulation or assimilation in the future.

4. What does "Observation Proportion" mean in Table 1?

Response: We apologize for the confusion. The phrase "Observation Proportion" has been changed to "Algorithms without observation rejection". We also add some details related to this type of experiments to Section 2.5.

5. Which version of MODIS LAI collection did you use?

Response: Global Land Surface Satellite (GLASS) LAI dataset is used in this study as observations for assimilation (Zhao et al., 2013). Since the ensemble simulation or assimilation is run at the resolution of 0.9° latitude by 1.25° longitude, the original

spatial resolution of 0.05° of GLASS LAI is upscaled to the same resolution. To evaluate the assimilation result, an improved LAI dataset developed from the MODerate Resolution Imaging Spectroradiometer (MODIS) (Yuan et al., 2011) is utilized, which can reduce the spatial and temporal inconsistencies by considering the characteristics of the MODIS LAI data and quality control (QC) information (Baret et al., 2013). The resolution of MODIS LAI is 1-km, which is upscaled to grid level to evaluate the analysis of LAI and assimilation effect. Section 2.4.2 is newly added to the revised manuscript.

6. There is no legend in Figure 1. Please add.

Response: Figure 1 is improved and legend is added to the revised manuscript.

7. Due to the impacts of cloud cover, aerosols, snow cover, and sensor failure, MODIS LAI products are characterized by high noise, low accuracy, and large fluctuations in the time series. By calculating the RMSE of assimilation/simulation LAI and MODIS LAI, can this paper really choose a better assimilation algorithm?

Response: To evaluate the assimilation result, an improved LAI dataset developed from the MODerate Resolution Imaging Spectroradiometer (MODIS) (Yuan et al., 2011) is utilized, which can reduce the spatial and temporal inconsistencies by considering the characteristics of the MODIS LAI data and quality control (QC) information (Baret et al., 2013). The resolution is 1-km, which is upscaled to the grid level to evaluate the analysis of LAI and assimilation effect. It is better evaluate the LAI estimation by using in-situ observations, but it is not possible to do so on global scale.

8. Lines 2-3 in page 11, “assimilated observation” is mean “assimilated LAI”?

Response: You are right. The sentence has been changed as suggested.

9. The legend and coordinate axis numbers are blurred in Figure 6.

Response: Figure 6 is corrected in the revised manuscript.

10. “the distribution characteristics of both innovations and residuals are identical for the algorithms of KF and PF, which means that these two algorithms are not very efficient for LAI assimilation.” Why innovations and residuals are identical, KF and PF are invalid. However, both innovations and residuals are not exactly the same for the algorithms of KF and PF ((g) and (h), (o) and (p) in Figure 6).

Response: The word “identical” is changed to “similar”; furthermore, Figure 6 has been improved in the revised manuscript.

11. How to calculate the proportion of accepted LAI observations?

Response: During assimilation, the DART can calculate the number of non-assimilated

observations when the difference of the prior mean and observations is larger than three times of the expected value. The proportion of accepted LAI observations is defined as the number of accepted observations divided by the number of total observations.

12. lines 3-4 in page 13, what are the conditions that observations are rejected during data assimilation.

Response: The "Algorithms" experiments would reject some observations under certain conditions using the KF, EnKF, EAKF, and PF algorithms. The expected value of the difference between the prior mean and observations is $\sqrt{\sigma_{\text{prior}}^2 + \sigma_{\text{obs}}^2}$, in which σ_{prior} and σ_{obs} are standard deviations of prior PDF and observation PDF respectively. DART will reject the observation if the bias of the prior mean and observation is larger than three times of the expected value.

13. lines 13-14 in page13, is RMSE calculated by EAKF_noreject/EAKF_reject and MODIS LAI?

Response: correct. The sentence has been changed as suggested.

Interactive comment on "Comparison of Different Sequential Assimilation Algorithms for Satellite-derived Leaf Area Index Using the Data Assimilation Research Testbed (lanai)" by Xiao-Lu Ling et al.

Anonymous Referee #2

Received and published: 25 March 2019

1 OVERVIEW

The paper proposes to compare the performance of four data assimilation (DA) algorithms in assimilating GLASS LAI within the CLM4CN land surface model (LSM) using the DART toolbox (version lanai). The four algorithms are: the Kalman filter (KF), an Ensemble Kalman Filter (EnKF), the Ensemble Adjustment Kalman Filter (EAKF) and a particle filter (PF). The authors show that the EAKF produces LAI estimates that are the closest to the assimilated observations. They also study the influence of observation selection on LAI estimates compared to assimilated observations.

2 GENERAL COMMENTS

The objective of comparing assimilation methods for assimilating LAI in Land Data Assimilation Systems (LDASs) is fair and the choice of the various methods looks sound. The work belongs to a now long list of papers comparing DA methods in LDASs, most of them focusing on soil moisture. The novelty of the paper lies in the comparison of several DA methods assimilating LAI on global scale. Unfortunately the paper in its current form suffers from several issues that prevent it to be published as is. In particular:

• I think your results lack of analysis and validation. You only focus on assimilating GLASS LAI and compare newly LAI estimates with assimilated observations by computing RMSE. By using this sole criterion, you may miss something. The following analyses are missing:

1. – The paper misses an analysis on the evolution of variances or ensemble spread of your LAI estimates.

Response: Thank you for your suggestion. The RMSEs of the ensemble members are showed in Figure 3 to provide the hints where the assimilation is the most efficient. Please see Figure 3.

2. – You only focus on estimated LAI but your state vector also include Leaf C and

Leaf N. How do these two variables evolve in time with DA?

Response: In the former experiment, considering the large file size and limited storage capacity, we only output LAI. In the future, we can re-run the ensemble assimilation or simulation and output more variables if the storage capacity is increased.

3. – You do not validate your approach with independent datasets. To validate a DA system, it is usual to compare control variables or other variables to independent datasets in order to check if assimilation has a positive impact. I suggest you use in-situ observations of LAI or use satellite estimates of evapotranspiration or gross primary production (estimates of both quantities have been shown improved by assimilating LAI) that are independent from the GLASS LAI product to validate your approach more thoroughly.

Response: To evaluate the assimilation result, an improved LAI dataset developed from the MODerate Resolution Imaging Spectroradiometer (MODIS) (Yuan et al., 2011) is utilized, which can reduce the spatial and temporal inconsistencies by considering the characteristics of the MODIS LAI data and quality control (QC) information (Baret et al., 2013).

• Too many details in the description of the experimental setup are missing. For example:

4. – Which period of time does your experiment cover? You have atmospheric forcing covering the period 1998-2010 but you only show results for the year 2002. Does that mean your experiment only cover one year? If so, this is not enough to determiner seasonal tendencies. Adding another year of experiment would reinforce your conclusions. If your experiment covers more than a year, please show results for the other years.

Response: 80 atmospheric forcing datasets at 6-hour intervals over the period of 1998-2010 are used in this study. Considering the computational cost and filter performance, only 40 members are randomly selected. The reasons why the time of LAI in the result is 2002 are given below. First, the ensemble simulation during the time period of 1998 ~ 2001 is treated as spin-up. A detailed description of the spin-up process has been added to Section 2.5 in the revised manuscript. Second, the purpose of this study is to find out the optimal algorithm, which means that many experiments need to be conducted. Aiming at global scale and considering the computational cost, only one-year assimilation and ensemble simulation are conducted. We try to first find out the best experiment, and then conduct long-term simulation or assimilation in the future.

5. – At which resolution do your run CLM4CN? In Figure 1, you show pictures at 1.0_

resolution. Does that mean you run your LSM at the same resolution? Also, I thought that the GLASS LAI dataset was available at 0.05_ resolution. Do you do interpolation in order to create the LAI you assimilate?

Response: The ensemble simulation or assimilation is run at the resolution of 0.9° latitude by 1.25° longitude. Therefore, the original spatial resolution of 0.05° of GLASS LAI is upscaled to the same resolution.

6. – What kind of criterion do you use for observation selection? Is it when "the observed LAI is three times larger than the bias between the simulation and the observations" (l 16-17, p. 13)?

Response: The expected value of the difference between the prior mean and observations is $\sqrt{\sigma_{prior}^2 + \sigma_{obs}^2}$, in which σ_{prior} and σ_{obs} are standard deviations of prior PDF and observation PDF, respectively. DART will reject the observation when the bias of prior mean and observation is larger than three times of the expected value.

I know it is impossible to include every detail in a paper or in supplementary materials. But I would like to remind the authors that every reader should be able to reproduce the experiment you conducted after reading a paper. In current form, your paper does not satisfy this important criterion.

• Too many details are also missing in the description of the DA methods you use.

7. – I suspect your DA system works pointwise meaning you do not consider spatial covariances in KF, EnKF and EAKF. This is a strong hypothesis (perfectly respectable one). Could you confirm or reject my claim? If true, you should emphasize that point in your paper. If not, the whole analysis of spatial covariances is missing.

Response: We have further discussed this issue in the revised manuscript. Please see Section 2.5.

8. – Could you recall in the paper the different equations involved for each DA method you use? Since it is a paper that compares various DA methods, the reader would benefit from having those written.

Response: Thank you for your suggestion. We have recalled the equations in the revised manuscript.

9. – From what I read, it is impossible to determine which version of the particle filter you are using. Do you use the traditional Sequential Importance Resampling (SIR)

filter from Gordon et al. (1993) or do you use more evolved techniques to counteract the degeneracy of the particle filter?

Response: Following recommendations in the DART tutorial, the traditional Sequential Importance Resampling (SIR) filter from Gordon et al. (1993) is used in this study. Note that we didn't do anything to counteract the degeneracy of the particle filter.

10. – To run each member of your ensemble, you use 40 different atmospheric forcings selected from the 80-members DART/CAM4 dataset. How do you select them? Are they representative of the spread (uncertainty) of the whole 80-members atmospheric forcing dataset? If you select them randomly, you may have under-sampling issues (increasing the risk of filter divergence either for EnKF, EAKF and PF). Could you elaborate more on that subject?

Response: 40 different atmospheric forcing datasets are selected randomly. Considering the computational cost and the EAKF performance (e.g., Reichle et al., 2002; Zhang et al., 2014), it is not necessary to conduct the assimilation with 80 atmospheric forcing datasets. The ensemble atmospheric forcing should be designed identical for the four experiments for the purpose to find out the optimal algorithm. Furthermore, investigating uncertainties caused by different meteorological forcing datasets is beyond the scope of this study.

11. – Ensemble Kalman Filters (either what you call EnKF and EAKF) underestimate systematically variances. What do you do to counteract this problem? Do you use inflation (additive, multiplicative)? If so, how? If not, why?

Response: We didn't do any inflation because the objective of the present study is to compare the performance of different algorithms provided by DART under the same condition. For this reason, we use the default settings in DART except for the algorithm.

As you can see the list of my comments is quite long. I do detail few of them in the next section. Nevertheless, I still consider the paper worth to be published if all points are addressed and, therefore, ask for a major revision.

3 SPECIFIC COMMENTS

1. • About the (lanai) in the title, could you make it more explicit that lanai is a version of DART in the title? It is confusing for the reader if she/he does not know what DART is.

Response: Thank you for your suggestion. We have changed the description from " DART (lanai)" to "DART (version Lanai)".

2. • p. 1, l. 13-14, “To improve the ability to simulate land surface water and energy balances”, since you show nothing related land surface water or energy fluxes, I suggest you to remove that comment.

Response: As suggested, this sentence has been deleted.

3. • p. 1, l. 23, “The PF algorithm performs worse than the EAKF and EnKF : : :”. You only consider RMSE as a criterion using for the PF the sampled mean. While using the mean makes sense for Ensemble Kalman Filters, for PF you have more freedom, one could use the particle with the biggest weight (a posteriori maximum for the pdf) for example. Could you add nuance to this statement?

Response: As suggested, we have added this statement to the revised manuscript.

4. • The introduction tends to mix general DA references to LDAS references making unclear for reading. I suggest you split your review in different paragraphs, one dedicated to DA in general, one dedicated to LDASs and one to the assimilation of LAI. Also many references are missing. Among others:
   – for DA in general: Bannister (2016), Vetra-Carvalho et al. (2018),
   – for LDASs: Lahoz and De Lannoy (2014), Reichle et al. (2014), De Lannoy et al. (2016), Sawada et al. (2015), Sawada (2018)
   – for assimilation of LAI: Sabater et al. (2008), Ines et al. (2013), Jin et al. (2018), Fox et al. (2018)
   Those references should help you build a thorough introduction.

Response: Thank you for your suggestion. The introduction has been improved in the revised manuscript. We also added many new references to this section, including those you mentioned.

5. • In section 2.2, can you recall that you use the lanai version of DART?

Response: The subtitle has been changed from “DART” to “DART (the Lanai version)”. We also added some details to Section 2.2.

6. • Section 2.3.1 about the Kalman Filter (KF). The KF can only be used if your model is linear. Is your LSM linear between two times of observations (roughly 8 days)? If so please indicate what makes CLM4CN linear (as most LSMs are not!). If not, what you are using is rather an Extended Kalman Filter (EKF), in that case, how do you propagate the error covariance matrix from one time of observation to another i.e. how do you calculate the Jacobian matrix of your model?

Response: Thank you very much for your suggestion. Generally speaking, the CLM4CN is nonlinear, so the Kalman Filter could not be used for the LSMs. We have

checked the DART tutorial, and found that the algorithm we used in this study is the Ensemble Kernel Filter (EKF). We apologize for this mistake, and the detailed information about the EKF has been added to Section 2.3.1.

7. • Section 2.3.2 about the Ensemble Kalman Filter. What you call the Ensemble Kalman Filter (EnKF) is likely the stochastic Ensemble Kalman Filter introduced by Burgers et al. (1998) and Houtekamer and Mitchell (1998) meaning that observations are perturbed for each member of the ensemble. Could you confirm it? And if so, please refer to those two papers.

Response: As suggested, we have added this information to Section 2.3.2. The references are also added to the revised manuscript.

8. • p. 5, l. 33. Eq (1) is false. The denominator of the fraction should be $\sigma_o^p + \sigma_{j_o}^p$.

Response: Thank you for your information. We have corrected the equation.

9. • p. 6, l. 8. The variables involved in Eq. (2) are not defined.

Response: If there are enough observations, the posterior density at k can be approximated by

$$p(X_k^a|Y_{1:k}) \approx \sum_{i=1}^{N} w_{i,k}\, \delta(X_k^a - X_{i,k}^a)$$

in which $\delta(*)$ is the Dirac Function and $\sum_{i=1}^{N} w_{i,k} = 1$. $p(X_k^a|Y_{1:k})$ is the posterior probability distribution, $X_{i,k}^a$ is the particle element, $w_{i,k}$ is the weight of each particle, N is the number of particles.

10. • Section 2.5. You put Table 1 in section 2.5 but there is no mention in the text of the observation proportion you perform. Could you add sentences on that subject in section 2.5?

Response: We apologize for the confusion. We have changed the phrase from "Observation Proportion" to "Algorithms without observation rejection". We have also added some details related to this type of experiment to Section 2.5.

11. • p. 6, l. 29. You refer to the GLASS LAI dataset but afterwards you instead call them MODIS LAI. While I know GLASS LAI is from MODIS from 2002, it is rather confusing. Could you harmonize your notation?

Response: Global Land Surface Satellite (GLASS) LAI dataset is used in this study as observations for assimilation (Zhao et al., 2013). As the ensemble simulation or assimilation is run at the resolution of 0.9° latitude by 1.25° longitude, the original spatial resolution of 0.05° of GLASS LAI is upscaled to the same resolution. To

evaluate the assimilation result, an improved LAI dataset developed from the MODerate Resolution Imaging Spectroradiometer (MODIS) (Yuan et al., 2011) is utilized, which can reduce the spatial and temporal inconsistencies by considering the characteristics of the MODIS LAI data and quality control (QC) information (Baret et al., 2013). The resolution is 1-km, which is also upscaled to the grid level to evaluate the analysis of LAI and assimilation effect. We also added section 2.4.2 to the revised manuscript.

12. • p. 7, Fig 1. There is no scale for Figure 1

Response: Figure 1 has been improved in the revised manuscript.

13. • p. 8, l. 5-6. "Figure 4 presents the root mean square errors (RMSEs) : : :" Strictly speaking, they are not RMSEs but RMSDs (root-mean square differences) since your observations are not perfect. Please replace RMSE by RMSD.

Response: Thank you for your suggestion. All the RMSEs in this manuscript have been changed into RMSDs.

14. • p. 10, Fig. 4 It looks like the assimilation is far less efficient in the boreal area than in other places. Can you explain why?

Response: The assimilation is far less efficient in the boreal region than in other areas, which is partly attributed to the consistently low initial RMSD during non-growing seasons and limited capability of the model to simulate processes associated with boreal forest types.

15. • p. 10, Fig 5. The RMSE for EnKF is not consistent to what is shown in Fig 4 (EnKF and EAKF give close results). Can you explain why?

Response: There are some misunderstandings in Fig.5, in which the RMSD for EAKF is the value for the EAKF_noreject experiment, while the RMSDs for the other three algorithms are the ones from the reject experiments. We apologize for the confusion, and we have improved Fig. 5 in the revised manuscript. Furthermore, we have added new values to compare the difference of RMSDs between EAKF_noreject and EAKF_reject experiments, which are discussed in Section 4.

16. • p. 11, Fig 6. I cannot read the figure. Can you make it bigger?

Response: Figure 6 is corrected in this revision.

17. • p. 13, Fig 8. Have you compared LAI estimates (when you use observation selection) with every obs of LAI or only with those selected? It is rather normal that RMSDs are larger when you do not assimilate every observation than when you do. It would be worth comparing LAI estimates (when you use/do not use observation

selection) with the selected observations only and see if you obtain smaller RMSDs.

Response: Thank you for your suggestion. Figure 9 shows the RMSDs of simulation experiments without/with rejection (EAKF_noreject and EAKF_reject) and MODIS LAI for the globe and subregions. We have added details to revised manuscript.

4 REFERENCES

Bannister, R. N.: A review of operational methods of variational and ensemble variational data assimilation, Q. J. R. Meteorol. Soc., 143, 607-633, 2016.

Burgers, G., van Leeuwen, P. J. and Evensen, G.: Analysis scheme in the ensemble Kalman filter, Mon. Wea. Rev., 126, 1719-1724, 1998.

Houtekamer, P. L. and Mitchell, H. L.: Data assimilation using an ensemble Kalman filter technique, Mon. Wea. Rev., 126, 796-811, 1998.

De Lannoy, G. J. M., de Rosnay, P. and Reichle, R. H.: Soil moisture data assimilation. In Handbook of Hydrometeorological Ensemble Forecasting, edited by Q. Duan, F. Pappenberger, J. Thielen, A.Wood, H. Cloke and J. C. Schaake. 2016.

Fox, A. M., Hoar, T. J., Anderson, J. L., Arellano, A. F., Smith, W. K., Litvak, M. E., et al.: Evaluation of a data assimilation system for land surface models using CLM4.5. Journal of Advances in Modeling Earth Systems, 10, 2471-2494, 2018.

Gordon, N. J., Salmond, D. J. and Smith, A. F.: Novel approach to nonlinear/non-Gaussian Bayesian state estimation, IEE Proc., 140, 107-113, 1993.

Ines, A. V. M., Das, N. N., Hansen, J. P. and Njoku, E. G.: Assimilation of remotely sensed soil moisture and vegetation with a crop simulation model for maize yield prediction, Remote Sensing of Environment, 138, 149-164, 2013.

Jin, X., Kumar, L., Li, Z., Xu, X., Yang, G. and Wang, J.: A review of data assimilation of remote sensing and crop models, Eur. J. Agron., 92, 141-152, 2018.

Lahoz, W. A. and De Lannoy, G. J. M.: Closing the Gaps in Our Knowledge of the Hydrological Cycle over Land: Conceptual Problems, Surv. Geophys., 35, 623-660, 2014.

Reichle, R. H., De Lannoy, G. J. M., Forman, B. A., Draper, C. S. and Liu, Q.: Connecting Satellite Observations with Water Cycle Variables Through Land Data Assimilation: Examples Using the NASA GEOS-5 LDAS, Surv. Geophys., 35, 577-606, 2014.

Sabater, J. M., Rüdiger, C., Calvet, J.-C., Fritz, N., Jarlan, L. and Kerr Y.: Joint assimilation of surface soil moisture and LAI observations into a land surface model, Agr. Forest Meteorol., 148, 1362-1373, 2008.

Sawada, Y., Koike, T. and Walker, J. P.: A land data assimilation system for simultaneous simulation of soil moisture and vegetation dynamics. J. Geophys. Res. Atmos., 120, 5910-5930, 2015.

Sawada, Y.: Quantifying Drought Propagation from Soil Moisture to Vegetation Dynamics Using a Newly Developed Ecohydrological Land Reanalysis, Remote Sens., 10, 1197, 2018.

Vetra-Carvalho, S., van Leeuwen, P. J., Nerger, L., Barth, A., Altaf, M. U., Brasseur, P. Kirchgessner, P. and Beckers, J.-M.: State-of-the-art stochastic data assimilation methods for high-dimensional non-Gaussian problems, Tellus A, 70, 1445364, 2018.

Response: Thank you for the kind information. We have added these references to the revised manuscript.

Comparison of Different Sequential Assimilation Algorithms for Satellite-derived Leaf Area Index Using the Data Assimilation Research Testbed (Version Lanai)

Xiao-Lu Ling [1,2,3], Cong-Bin Fu [1,2,*], Zong-Liang Yang [3,*], and Wei-Dong Guo [1,2]

[1]Institute for Climate and Global Change Research & School of Atmospheric Sciences, Nanjing University, Nanjing 210023, China

[2]Joint International Research Laboratory of Atmospheric and Earth System Sciences of Ministry of Education, Nanjing 210023, China

[3]Department of Geological Sciences, John A. and Katherine G. Jackson School of Geosciences, University of Texas at Austin, Austin, TX 78705, USA

Correspondence to: Cong-Bin Fu (fcb@nju.edu.cn); Zong-Liang Yang (liang@jsg.utexas.edu)

Abstract. The leaf area index (LAI) is a crucial parameter for understanding the exchanges of momentum, carbon, energy, and water between terrestrial ecosystems and the atmosphere. In this study, the Data Assimilation Research Testbed (DART) has been successfully coupled to the Community Land Model (CLM) by assimilating global remotely sensed LAI data with explicit carbon and nitrogen components (CLM4CN). The purpose of this paper is to determine the best algorithm for LAI assimilation. Within this framework, four sequential assimilation algorithms, i.e., the Kernel Filter (KF), the Ensemble Kalman Filter (EnKF), the Ensemble Adjust Kalman Filter (EAKF), and the Particle Filter (PF), are applied, thoroughly analysed and compared. The results show that assimilating remotely sensed LAI data into the CLM4CN is an effective method for improving model performance. In detail, the assimilation accuracies of the ensemble filter algorithms (EnKF and EAKF) are better than that of the KF algorithm because the KF is based on the linear model error assumption. From the perspective of average and RMSE, the PF algorithm performs worse than the EAKF and EnKF algorithms because of the gradually reduced acceptance of observations with assimilation steps. In other words, the contribution of the observations to the posterior probability during the assimilation process is reduced. The EAKF algorithm is the best method because the matrix is adjusted at each time step during the assimilation procedure.

1 Introduction

Land surface processes play an important role in the earth system because all the physical, biochemical, and ecological processes occurring in the soil, vegetation, and hydrosphere influence the mass and energy exchanges during land-atmosphere interactions (Bonan, 1995; Pitman, 2003; Pitman et al., 2009, 2012). The leaf area index (LAI) is a key biophysical parameter of vegetation in land surface models (LSMs) and influences their simulation performance. Therefore, high-quality, spatially and temporally continuous LAI inputs are extremely important (Bonan et al., 1992; Li et al., 2015).

Deleted: lanai

Deleted: To improve the ability to simulate land surface water and energy balances

Deleted: Kalman

Deleted: analyzed

Deleted: The

Formatted: Indent: First line: 2 ch

Real-time monitoring of LAI on a large scale is a worldwide problem. The lack of spatial representativeness caused by the sparse distribution of conventional observations makes it difficult to achieve a global observational LAI dataset. Remote sensing can provide global data with high spatial and temporal resolutions, but the inversion accuracy is associated with different plant functional types (PFTs) and vegetation fractions. Furthermore, although advanced land surface models (LSMs, e.g., the Community Land Model version 4, CLM4) can predict LAI variation, the model performance is greatly affected by the model structure or the initial/forcing/boundary conditions of the input (Dai et al., 2003; Luo et al., 2003; Levis et al., 2004). Data Assimilation (DA), through optimally combining both dynamical and physical mechanisms with real-time observations, can effectively reduce the estimation uncertainties caused by spatially and temporally sparse observations and poor observed data accuracy (Kalnay, 2003).

As a link between observations and dynamic model states, mathematical algorithms play an important role in calculating the increments and adjusting the state vector during assimilation (Kalnay et al., 2007). The two basic data assimilation algorithms are the variational DA based on optimal control theory and sequential algorithms based on the Kalman Filter (KF) (Dimet and Talagrand, 1986; Gordon et al., 1993; Bannister et al., 2017; Vetra-Carvalho et al., 2018). Because the KF algorithm is based on the linear model error assumption, many new sequential algorithms have been proposed. For example, the Extended Kalman Filter (EKF) was developed to meet the need for a nonlinear observation operator, but the tangent operator needs to be developed (Kalnay, 2003). Based on the Monte Carlo method and focused on the nonlinear operator, the Ensemble Kalman Filter (EnKF) was developed (Evensen, 1994) and was first used in the study of atmospheric science (Houtekamer and Mitchell, 1998). Since then, the EnKF has been widely applied for the assimilation of ocean, land surface and atmospheric data (Houtekamer et al., 2005; Evensen, 2007). In recent years, the Monte-Carlo methods have been proposed to allow the assimilation of information from sources that have non-Gaussian errors.

Many previous studies focusing on the comparison of variational and sequential algorithms have been conducted to determine the optimal assimilation method (Han and Li, 2008). Wu et al. (2011) systematically compared EnKF and 3DVAR/4DVAR algorithms and found that the EnKF algorithm was better than the 3DVAR method and the same as the 4DVAR method. For this reason, the application of the EnKF algorithm has been expanded quickly, and many other forms of the EnKF method have been developed, such as the Dual EnKF (Li et al., 2014), Ensemble Square Root Filter (EnSRF) (Whitaker and Hamill, 2002), and Ensemble Adjust Kalman Filter (EAKF, Anderson, 2001). At the same time, combinations of variational algorithms and sequential algorithms have also been developed. For example, the maximum likelihood ensemble filter (MLEF, Zupanski, 2005), the combination of 3DVAR and PF algorithms (Leng and Song, 2013), the hybrid variational-ensemble data assimilation methods, i.e., the 4DEnKF (Hunt et al., 2004; Fertig et al., 2007; Zhang et al., 2009) and the DrEnKF (Wan et al., 2009) have been developed at NCEP and applied to improve model predictions (Whitaker et al., 2008).

A complete Land Data Assimilation System (LDAS) is mainly composed of forcing datasets, initial and boundary datasets, parameterization sets, dynamical models as physical constraints, assimilation algorithms, observational data and target output. In recent decades, studies of land data assimilation have become very active, although this topic was proposed later than the assimilation of atmospheric

Deleted: (

Deleted: The Land

Deleted: System (LDAS

Deleted: A complete LDAS is mainly composed of forcing, initial and boundary datasets, parameterization sets, dynamical models as physical constraints, assimilation algorithms, observational data and target output.

Moved down [1]: The widely acknowledged LDASs include the North LDAS (NLDAS, Mitchell et al., 2004; NLDAS-2, Luo et al., 2003; Xia et al., 2012),

Deleted: Global LDAS (GLDAS, Rodell et al., 2004), European LDAS (ELDAS, Jacobs et al., 2008), West China LDAS (WCLDAS, Huang and Li, 2004), and

Moved down [2]: Canadian LDAS (CaLDAS, Carrera et al., 2015).¶

Deleted: method based on optimal control theory (Dimet and Talagrand, 1986) and sequential algorithms based on the Kalman Filter (KF). To date, the most popular variational algorithms widely utilized in LDAS (Evensen, 2003) are three-dimensional variation (3DVAR, Zhang et al., 2011) and four-dimensional variation (4DVAR) algorithms. For 3DVAR algorithms, the observation operator can be nonlinear, but the background variance is isotropic and does not change with time. The 4DVAR algorithms can employ flow-dependent forecast error covariance but cost more to implement and maintain. The state quantity is estimated by using all possible observations and the statistical characteristics of dynamic model simulations and observations to minimize the estimated error. The KF is the theoretical basis of the sequential data assimilation algorithm.

Deleted:) was developed to find

Deleted: optimal solution by minimizing the target function for the nonlinear observation operator. The

Deleted: also showed better results than either single algorithm

Deleted:). Furthermore,

Deleted:),

observations (Lahoz and De Lannoy, 2014). Land data assimilation can implement both in-situ observations and remotely sensed data like satellite observation of soil moisture, snow water equivalent (SWE), land surface temperature and so on to constrain the physical parametrization and initialization of land surface state. (Liu et al., 2008; Reichle et al., 2014; Zhang et al., 2014; Zhao et al., 2016; 2018). The widely acknowledged LDASs include the North LDAS (NLDAS, Mitchell et al., 2004; NLDAS-2, Luo et al., 2003; Xia et al., 2012), the Global LDAS (GLDAS, Rodell et al., 2004), the European LDAS (ELDAS, Jacobs et al., 2008), the West China LDAS (WCLDAS, Huang and Li, 2004) and the Canadian LDAS (CaLDAS, Carrera et al., 2015).

Recent studies focusing on assimilation in terrestrial systems have tended to add multiple phenological observations to constrain and predict biome variables and further improve model performance (Knyazikhin et al., 1998; Xiao et al., 2009; Viskari et al., 2015). Joint assimilation of surface incident solar radiation, soil moisture and vegetation dynamics (LAI) into land surface models or crop models is of great importance since it can improve the model results for national food policy and security assessments (Sabater et al., 2008; Ines et al., 2013; Sawada et al., 2015; Jin et al., 2018; Mokhtari et al., 2018). Furthermore, the abilities to simulate river discharge, land evapotranspiration, and gross primary production have been improved in Europe (Barbu et al., 2011; Albergel et al., 2017). To date, such studies have been conducted using a single sequential algorithm at a single site or on regional scales (Montzka et al., 2012; Sawada et al., 2018).

The Data Assimilation Research Testbed (DART) is an open source community facility and includes several different types of KF algorithms (Anderson et al., 2009). It has been coupled to many high-order models and observations for ocean, atmosphere, land surface, and chemical constituents. For example, DART has been coupled with CLM4 or CLM4.5 to improve snow and soil moisture estimations as well as land carbon processes (Zhang et al., 2014; Kwon et al., 2016; Zhao et al., 2016; Fox et al., 2018; Zhao et al., 2018). Utilizing coupled DART/CLM4, the Global Land Surface Satellite LAI (GLASS LAI) data are assimilated into the Community Land Model with carbon and nitrogen components (CLM4CN) in the present study to explore the optimal assimilation algorithm for model performance. The experimental design and different assimilation algorithms are described in Sect. 2. Section 3 describes the optimal algorithm for LAI assimilation, and the proportion of observations is discussed in Sect. 4. Conclusions and discussions are given in Sect. 5.

2 Data and Methodology

A complete LDAS is mainly composed of forcing/initial/boundary datasets, parameterization sets, dynamical LSMs, assimilation algorithms, observational data and target output. LSMs play an important role in the LDAS because they can add physical constraints to the control variables during assimilation. In addition, the simulation ability of LSMs can directly affect the output because they provide the associated uncertainty for assimilation.

Moved (insertion) [1]

Moved (insertion) [2]

Deleted: Assimilating satellite-derived LAI and soil moisture products using the Simplified Extended Kalman Filter (SEKF) or EAKF has a strong impact on the LAI data.

Formatted: Indent: First line: 2.5 ch

Deleted: (DART/

Deleted:)

Deleted: , LAI

Deleted: predictions

Deleted:).¶

2.1 CLM4CN

Developed by the National Center for Atmospheric Research (NCAR), the Community Land Model (CLM) can simulate energy, momentum and water exchanges between the land surface and the overlying atmosphere at each computational grid. The CLM is designed mainly for coupling with the atmospheric numerical model and providing the surface albedo (direct and scattered light within the visible and infrared bands), upward longwave radiation, sensible heat flux, latent heat flux, water vapor flux, and east-to-west and south-to-north surface stress needed by the atmospheric model. These parameters are controlled by many ecological and hydrological processes. The model can also simulate leaf phenology and physiological processes, as well as water circulation through plant pores. Ecological differences between vegetation types and thermal and hydrological differences between different soil types are also considered. Each grid cell can be covered by several different land use types. Each cell contains several land units, each land unit contains a different number of soil and snow cylindrical blocks, and each cylindrical block may contain several types of vegetation functions. The CLM employs 10 soil layers to resolve soil moisture and temperature dynamics and uses PFTs to represent subgrid vegetation heterogeneity (Oleson et al., 2010).

There are two ways to update LAI in CLM4. The LAI is treated as a diagnostic variable that is linearly interpolated from a 30-year averaged satellite dataset, and there is no annual LAI variation for CLM4 with Satellite Phenology (CLM4SP) (Lawrence and Chase, 2007). For CLM4CN, the prognostic LAI is calculated by the leaf carbon pool and an assumed vertical gradient of specific leaf area (SLA) (Thornton and Zimmermann, 2007). Carbon and nitrogen are obtained by plant storage pools in one growing season and then retained and distributed in the subsequent year. All carbon and nitrogen state variables in vegetation, litter, and soil organic matter (SOM) are prognostic based on the prescribed vegetation phenology. The CLM4CN offline mode with prescribed meteorological forcing is used in this study.

2.2 DART (the Lanai version)

DART is developed and maintained by the Data Assimilation Research Section (DAReS) at NCAR. The purpose of DART is to provide a flexible tool for data assimilation (DA), and it has been coupled with many 'high-order' models. As a software environment, DART makes it easy to explore a variety of data assimilation methods and observations with different numerical models. The DART system includes several different types of sequential algorithms, which are selected at runtime by a namelist setting. The Lanai version of DART, which supports many existing models including the CESM climate component, the MPAS (Model for Prediction Across Scales) models and the NOAH land model etc., is used in this study. Released in December 2013, the Lanai version of DART can process many new observation types and sources and include new diagnostic routines as well as new utilities. Detailed settings for DART can be found at https://www.image.ucar.edu/DAReS/DART/.

Deleted: The detailed

Currently, the coupled DART/CLM4 model has produced many reanalysis data for snow and soil moisture. It has been found that snow DA can improve temperature predictions, especially over the Tibetan Plateau, implying great implications for future land DA and seasonal climate prediction studies

(Lin et al., 2016). Furthermore, the coupled DART/CLM framework would be employed to assimilate other variables, such as LAI, from various satellite sources and ground observations (i.e., truly multi-mission, multi-platform, multi-sensor, multi-source, and multi-scale). Ultimately, this would allow earth system models to be constrained by all types of observations to improve model performance for seasonal and decadal prediction skills.

Deleted: multimission, multiplatform, multisensor, multisource, and multiscale).

2.3 Sequential Assimilation Algorithms

According to Anderson et al. (2001), Equation (1) is used to express how new sets of observations modify the prior joint state conditional probability distribution obtained from predictions based on previous observation sets.

$$\mathbf{p}(\mathbf{z}_{t,k}|\mathbf{Y}_{t,k}) = \mathbf{p}(\mathbf{y}^o_{t,k}|\mathbf{z}_{t,k})\,\mathbf{p}(\mathbf{z}_{t,k}|\mathbf{Y}_{t,k-1})/\,\mathbf{p}(\mathbf{y}^o_{t,k}|\mathbf{Y}_{t,k-1}) \quad (1)$$

in which $\mathbf{Y}_{t,k}$ *is defined as the superset of all observation subsets,* $\mathbf{y}^o_{t,k}$ is the *k*th subset of observations at time t, $\mathbf{z}_{t,k}$ is the joint state-observation vector for a given *t* and *k*. In ensemble applications, generally there is no need to compute the denominator of (1). Four algorithms for approximating the product in the numerator of (1) are presented below, and detailed information can be found in Anderson et al. (2001).

2.3.1 Ensemble Kernel Filter (EKF)

Deleted: Kalman

Deleted: KF

Deleted: As a theoretical basis of the sequential DA method, the aim of the KF is to achieve the optimal analysis field based on the variance minimization principle (Kalman, 1960). The main KF procedure is as follows: (1) During the forecast stage, the dynamical model produces the forecast variables and associated uncertainties at the next observation time step, and (2) at the analysis stage, updated analyzed variables and associated uncertainties are determined based on the previous information on the uncertainties for each ensemble member.¶
Compared with the statistical optimal interpolation algorithm, the predicted error changes with the dynamical model for the KF method. Furthermore, the KF method is more easily realized because the adjoint matrix is not needed. However, the KF method is based on the assumption of a Gaussian relation between the variables in the joint stage space prior distribution.¶

The kernel filter mechanism, first proposed by Lindgren et al. (1993) and further developed by Anderson and Anderson (1999), has been incorporated into the DART and can be extended to the joint state space. Detailed calculation process can be found in Anderson et al. (2001). The kernel filter is potentially general, because the values and expected values of the mean and covariance and higher-order moments of the resulting ensemble are functions of high-order moments of the prior distribution. However, when applied to large models, computational efficiency will be an issue for the application of the algorithm.

2.3.2 Ensemble Kalman Filter (EnKF)

The KF algorithm has not been widely used because of computing limitations and the linear model error assumption. The EnKF was proposed based on a Monte Carlo approximation, for which the background error covariance is approximated using an ensemble of forecasts (Evensen, 1994). The EnKF algorithm can be utilized for nonlinear systems and can also reduce the computing requirement of DA (Burgers et al., 1998; Evensen, 2003; 2007).

The EnKF procedure is divided into two stages: prediction and analysis. (1) In the prediction stage, the ensemble forecast field is generated from the ensemble initial condition, and the error covariance matrix of the ensemble forecast is calculated. (2) In the analysis stage, the simulation of each member of the ensemble is updated using the covariance matrix of observation vector error and state vector error. The traditional EnKF, an ensemble of Kalman Filters with each member using a different sample estimate of the prior mean and observations, is used in this study (Houtekamer and Mitchell1998).

2.3.3 Ensemble Adjust Kalman Filter (EAKF)

Although the forms of expression are different, the proposed EnSRF (Whitaker et al., 2002) and EAKF (Anderson, 2001) are the same algorithm.

The difference between the EAKF and the traditional EnKF lies in the adjustment of the gain matrix to avoid filtering the divergence problem by increasing the premise of the analysis error covariance (Anderson, 2003, 2007; Wang et al., 2007). In the EAKF algorithm, ensemble observation members are calculated by the observation operator, and the increment of each observation member is calculated as ΔY_i.

The increment ΔX_{ij} for each ensemble sample of each state variable in terms of ΔY_i can then be calculated as follows:

$$\Delta X_{ij} = \frac{\sigma_{j_o}^p}{\sigma_o^p + \sigma_{j_o}^p} \Delta Y_i. \quad (2)$$

where i indicates the ensemble member, j is the state vector member, $\sigma_{j_o}^p$ is the prior covariance of state vector and observation, and σ_o^p is the prior variance of observation.

2.3.4 Particle Filter (PF)

The Particle Filter (PF) is also a sequential Monte Carlo method, which is based on the Bayesian sequential importance sampling method (SIS). The PF algorithm finds a set of random samples in the state space to approximate the probability density function and then replaces the integral operation with the sample mean to obtain the process of minimum variance distribution of the state (Moradkhani et al., 2005). The procedure of the PF algorithm can also be divided into two frameworks: forecast and analysis.

If there are enough observations, the posterior density at k can be approximated as

$$p(X_k^a|Y_{1:k}) \approx \sum_{i=1}^{N} w_{i,k}\, \delta(X_k^a - X_{i,k}^a). \quad (3)$$

$\delta(*)$ is the Dirac Function and $\sum_{i=1}^{N} w_{i,k} = 1$.

in which $p(X_k^a|Y_{1:k})$ is the posterior probability distribution, $X_{i,k}^a$ is the particle element, $w_{i,k}$ is the weight of each particle, N is the number of particles. Unlike the EnKF algorithm, the PF method takes into account the weights of different particles and can be better applied to nonlinear systems. However, in association with the DA, there are a limited number of particles with large weights, and too many computing resources are distributed to particles with weights of approximately 0. This situation is called particle degradation (Doucet et al., 2000). Effective methods to solve this issue include resampling or selecting more reasonable importance functions.

2.4 Datasets

2.4.1 Ensemble Meteorological Forcing and initial conditions

The ensemble initial conditions and background error (Hu et al., 2014) are produced from ensemble analysis products generated by running DART and the Community Atmosphere Model (CAM4) (Raeder et al., 2012). DART/CAM4 produced 80 atmospheric forcing datasets with 6-hour time intervals for the

Formatted: Indent: First line: 2 ch

Deleted: $\frac{\sigma_{j_o}^p}{\sigma_o^p}$

Deleted: 1

Deleted: 2

period of 1998-2010. These ensemble meteorological data have been widely employed in DA for ocean, snow, soil moisture, and many other related studies (Danabasoglu et al., 2012). By considering computational cost and filter performance, 40 members among the ensemble forcing datasets are chosen to drive the CLM4CN.

To achieve a steady state solution for all state variables, the CLM4CN was run for 4000 years by Qian's forcing (*Qian et al.*, 2006) at the resolution of 1.9° latitude by 2.5° longitude (*Shi et al.*, 2013). Then the]. The CLM4CN was then forced by the ensemble mean of selected 40 members of DART/CAM datasets for 1000 years. In the last step, the ensemble simulation during the time period from 1998 to 2001 was treated as spin-up, and 40 ensemble initial conditions were obtained. Aiming at global scale and considering the computational cost, only one-year assimilation and ensemble simulation were conducted. Our goal is to first find out the best experiment, and then conduct long-term simulation or assimilation in the future.

2.4.2 LAI datasets

The Global Land Surface Satellite (GLASS) LAI dataset is used in this study as observations for assimilation (Zhao et al., 2013). Since the ensemble simulation or assimilation is run at the resolution of 0.9° latitude by 1.25° longitude, the original spatial resolution of 0.05° of the GLASS LAI is upscaled to the same resolution.

To evaluate the assimilation result, an improved LAI dataset developed from the MODerate Resolution Imaging Spectroradiometer (MODIS) (Yuan et al., 2011) is utilized. Spatial and temporal inconsistencies can be reduced by considering the characteristics of the MODIS LAI data and quality control (QC) information (Baret et al., 2013). The resolution of MODIS data is 1-km, which is also upscaled to the grid level to evaluate the analysis of LAI and assimilation effect.

2.5 Experimental Design

Table 1. Experimental design for LAI assimilation using DART/CLM4CN.

Experiment	Assimilated variables	Updated variables	Assimilation algorithm	Accept all observation
Algorithms	GLASS LAI	LAI, Leaf C, Leaf N	EAKF, EnKF, KF, PF	NO
Algorithms without observation rejection	GLASS LAI	LAI, Leaf C, Leaf N	EAKF	YES

To determine the optimal assimilation algorithm, five experiments corresponding to the KF, EnKF, EAKF and PF methods are designed and showed in Table 1, in which the "Algorithms" experiments would reject some observations under certain conditions using the KF, EnKF, EAKF, and PF algorithms. The expected value of the difference between the prior mean and observation is $\sqrt{\sigma_{prior}^2 + \sigma_{obs}^2}$, in which σ_{prior} and σ_{obs} are standard deviations of the prior PDF and observation PDF respectively. DART will reject the observation if the bias of the prior mean and observations is larger than three times of the

Formatted Table
Formatted: Font: +Body Asian (DengXian)
Deleted: YES
Deleted: Observation Proportion
Deleted: , EnKF, KF, PF
Deleted: NO
Deleted: four
Deleted: shown
Deleted: .

expected value. The "Algorithms without observation rejection" experiments would accept all the observed LAI. During assimilation, CLM stops and writes restart and history files at a frequency of 8 days. If there is available observational GLASS LAI data, they are assimilated into the CLM4CN. DART extract state vector, the increments are calculated by filtering at each time step, and the LAI, leaf carbon (Leaf C) and leaf nitrogen (Leaf N) are updated. The adjusted DART state vector is resent to the CLM restart files as a new initial condition for the next time step. All the simulation and assimilation are conducted at the spatial resolution of 0.9° latitude by 1.25° longitude. The ensemble assimilation is conducted pointwise, indicating that spatial covariances are not considered.

3 The Optimal Algorithm for DART/CLM4CN

The spatial distributions of global LAI in 2002 for (a) observations in July, (b) ensemble mean of simulations in July, (c) observations in November, and (d) ensemble mean of simulations in November are shown in Fig. 1. The observations in Fig. 1 are from the updated MODIS LAI dataset with a spatial resolution of 1.0 latitude by 1.0 longitude. There are two latitudinal belts of high LAI values located in the tropics and at 50-65°N. These two regions are mainly dominated by evergreen broadleaf forests and boreal forests, respectively. Because of the presence of deserts, plateaus and bare ground, the LAI is low in western North America, western Australia, southern Africa, and southern South America, where shrubs and/or grass are dominant. Globally, the CLM4CN can simulate the LAI distribution characteristics, except that it systematically overestimates LAI, especially at low latitudes. There are 3 high-LAI regions located in the tropics: the Amazon, central Africa, and some islands in Southeast Asia. The global LAI is lower in November than in July. The LAI values in the high latitudes of the northern hemisphere are higher in July than in November because November is not the growing season for most of the vegetation in the northern hemisphere.

Deleted: <*object*>

Deleted: Moderate Resolution Imaging Spectroradiometer (

Deleted:)

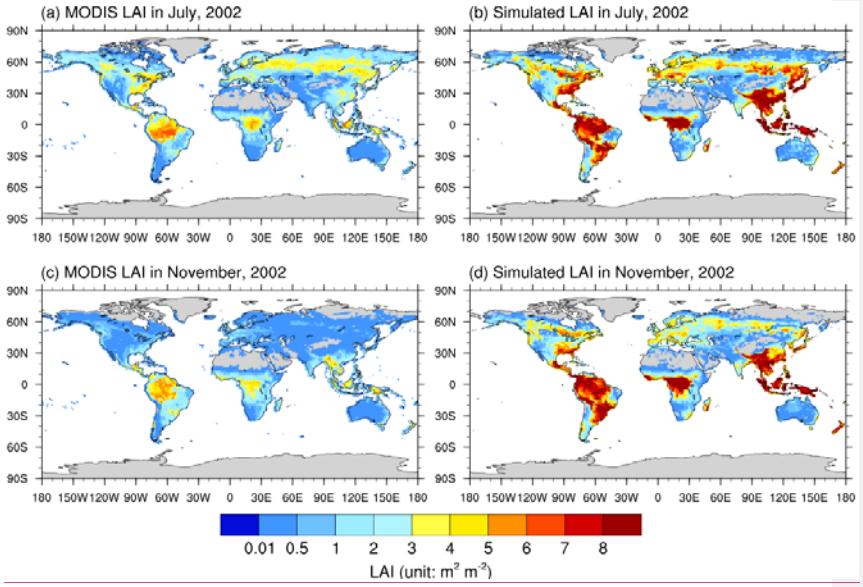

Figure 1: Spatial distributions of global LAI values in 2002 for (a) observations in July, (b) ensemble mean of simulations in July, (c) observations in November, and (d) ensemble mean of simulations in November.

The differences between global LAI from observations and that from assimilation experiments in July 2002 with the methods of (a) EAKF, (b) EnKF, (c) KF and (d) PF are shown in Fig. 2. Globally, assimilation results with the methods of EAKF and EnKF are larger in lower-latitude regions and higher-latitude regions in the Northern Hemisphere. For the EAKF and EnKF algorithms, large negative biases are located in the Amazon region, central Africa, and northeastern China, which are dominated by BET tropical, NET boreal forests and mixed forest types, respectively. The LAI values from the assimilation experiment are always higher in the middle- and high-latitude regions, especially in western North America, the northern Amazon, northwestern China, and western Australia, where open shrublands and grasslands are dominant. The LAI values from the assimilation experiments with the KF and PF algorithms are highly overestimated compared to the observations in the northern and eastern Amazon, central Africa, southern Eurasia, and Southeast Asia. In addition, the LAI values obtained by the EAKF method are more continuous than those obtained by the EnKF method and more consistent with the observations in central South America and central Africa. Notably, the correction of overestimated LAI is significantly better than that of underestimated LAI, which is mainly attributed to the high dispersion of LAI in those regions. In other words, high dispersion is beneficial to assimilation.

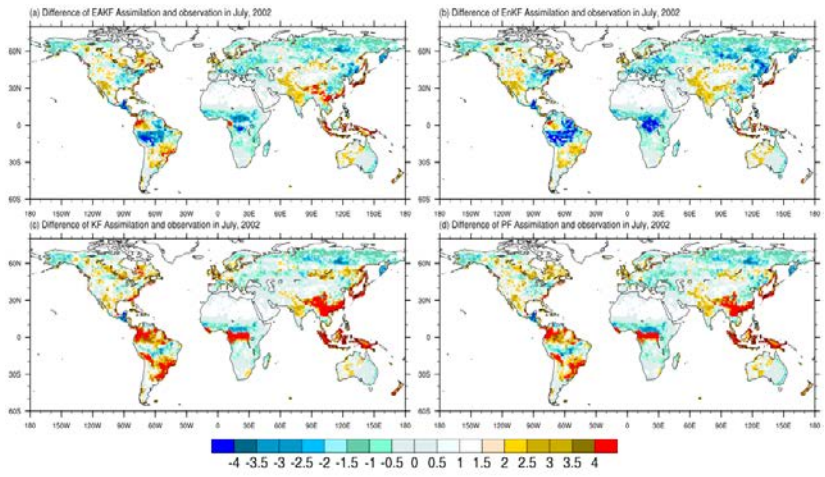

Figure 2: Differences between global LAI from assimilation experiments and that from observations in July 2002 with the methods of (a) EAKF, (b) EnKF, (c) KF and (d) PF.

The results also indicate that the EAKF and EnKF assimilation algorithms are better than the KF and PF algorithms in November (figures not shown). In detail, the EAKF algorithm is better than the EnKF method in November, especially in the Amazon, central Africa, and southern Eurasia. The biases of assimilated LAI relative to the observed LAI are higher in November in the 20-65°N region, which may be because vegetation during this period in the Northern Hemisphere is not lush. In western Australia and central Eurasia, the improvement of the underestimation in November is not as significant as that in

Deleted:

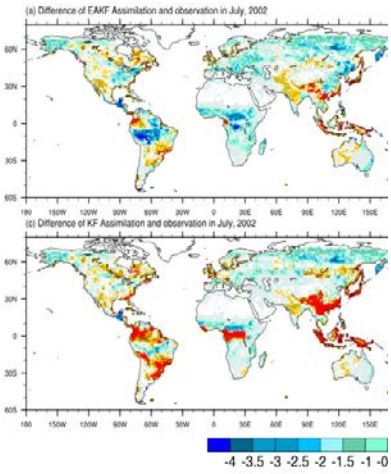

Deleted: differences between global observed LAI values and assimilated LAI values with the methods of (a) EAKF, (b) EnKF, (c) KF and (d) PF in November 2002 are also shown in Fig. 3. Similar to Fig. 2, the results

Deleted: .

July, which indicates that the system has a limited capability to simulate the vegetation process, especially for open shrubland and grassland. From the perspective of the average and RMSE, the PF algorithm performs worse than the EAKF and EnKF algorithms because of the gradually reduced acceptance of observations with assimilation steps. Note that the average and RMSE only make sense for the Ensemble Kalman Filters. For the PF algorithm, the particle with the largest weight (a posteriori maximum for the pdf) should be discussed separately.

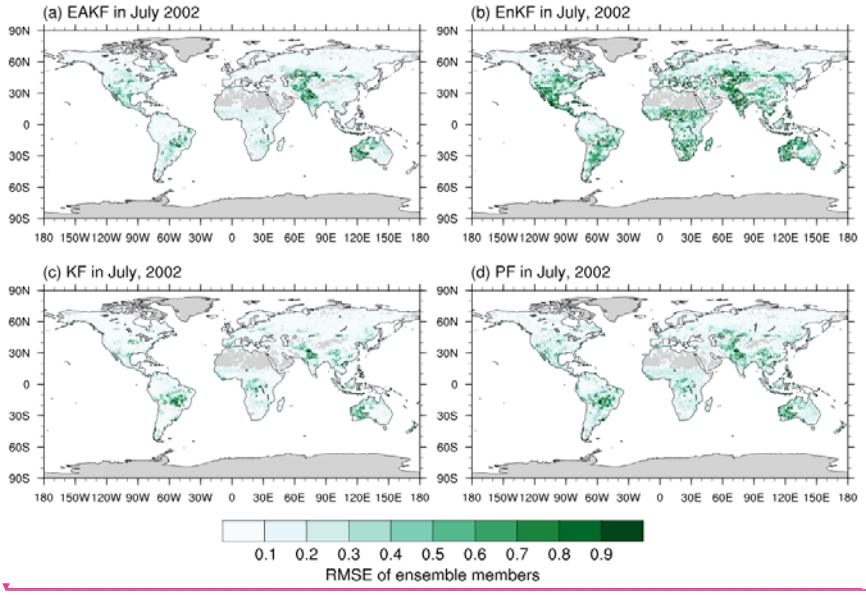

Figure 3: Same as Fig. 2, but for RMSE of ensemble members.

The RMSEs of ensemble members are showed in Figure 3 to provide hints where the assimilation is the most efficient. The RMSEs of ensemble members for the EAKF and EnKF algorithm are larger than those for the KF and PF algorithms, indicating that the EAKF and EnKF are more effective. In July 2002, the RMSE of the ensemble estimates is the largest in lower latitude regions, with particularly high values in central South America, central Africa, and Southeast Asia. The regions with comparatively large ensemble spreads are located in eastern North America and western Europe. The large ensemble spreads areas are also transitional regions with different vegetation types, indicating low capability of the models to simulate complex vegetation types.

The mean LAI globally and the LAI in five latitudinal bands were chosen for analysis in this study. The five bands are boreal (45-65°N), northern temperate (23-45°N), northern equatorial (0-23°N), southern equatorial (0-23°S), and southern temperate (23-90°S). Figure 4 presents the root mean square differences (RMSDs) of the ensemble means of simulation/assimilation versus observations for (a) global, (b) boreal, (c) northern temperate, (d) northern equatorial, (e) southern equatorial, and (f) southern temperate. Generally, although they all feature similar variation pattern characteristics, the RMSDs of all the assimilation datasets relative to the observations are less than those of the simulation, indicating that all four assimilation algorithms can improve the LAI simulation. The highest RMSD relative to the

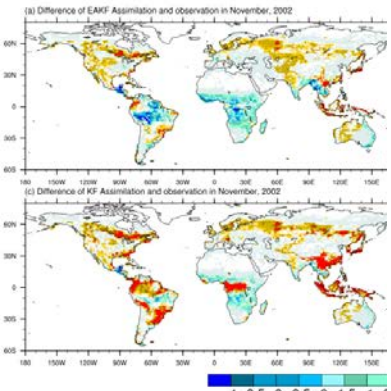

Deleted:

Deleted: November

Deleted: errors (RMSEs

Deleted: RMSEs

Deleted: RMSE

observations is associated with the simulation, followed by the assimilation datasets from the KF and PF algorithms, and the RMSDs are lowest for the EAKF and EnKF methods. During the growing season, the RMSDs of LAI reach their largest values, especially for the regions in the middle and high latitudes of the Northern Hemisphere and high latitudes of the Southern Hemisphere. In the low-latitude region covered by evergreen or deciduous broadleaf forests, the RMSD does not present an obvious annual change. Because the PF assimilation is heavily dependent on the weights of certain particles and to some degree ignores the importance of observed LAI data, the phenomenon of particle degradation occurs during the assimilation. The assimilation is far less efficient in the boreal region than in other areas, which is partly attributed to the consistently low initial RMSD during non-growing seasons and limited capability of the models for simulating processes associated with boreal forest type.

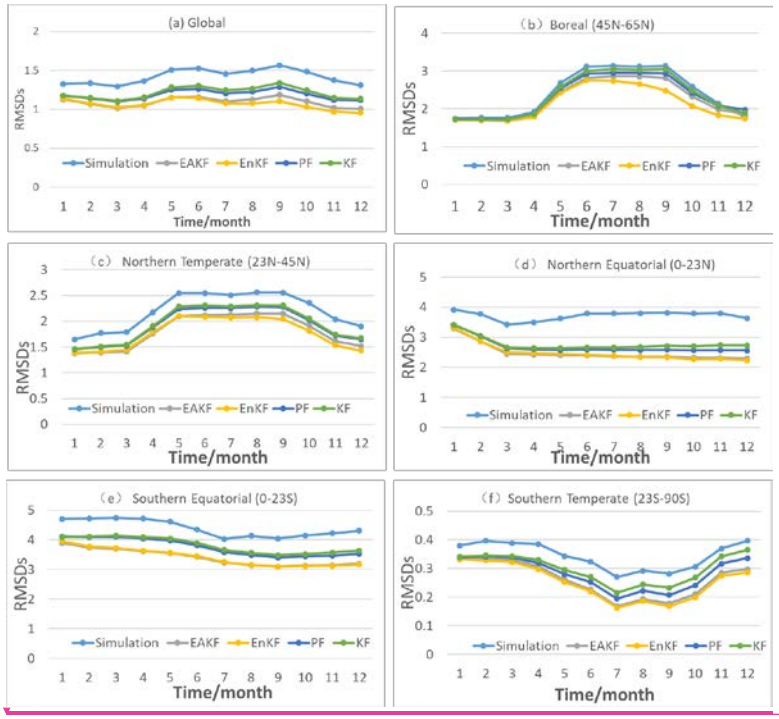

Figure 4: RMSDs of ensemble means of simulation/assimilation versus observations for (a) global, (b) boreal (45-65°N), (c) northern temperate (23-45°N), (d) northern equatorial (0-23°N), (e) southern equatorial (0-23°S), and (f) southern temperate (23-90°S).

Figure 5 shows the globally or regionally averaged RMSDs of simulation/assimilation and observations. The RMSDs of assimilation are lower than those of simulation, implying that assimilating remotely sensed LAI data into the CLM4CN is an effective method for improving the model performance. The RMSDs of assimilation results using the algorithms of EAKF and EnKF are much lower than the KF and PF methods, indicating their better performance in assimilation. The difference between simulation and all four algorithms in the northern and southern equatorial regions is larger than

Deleted: RMSEs

Deleted: RMSEs

Deleted: RMSE

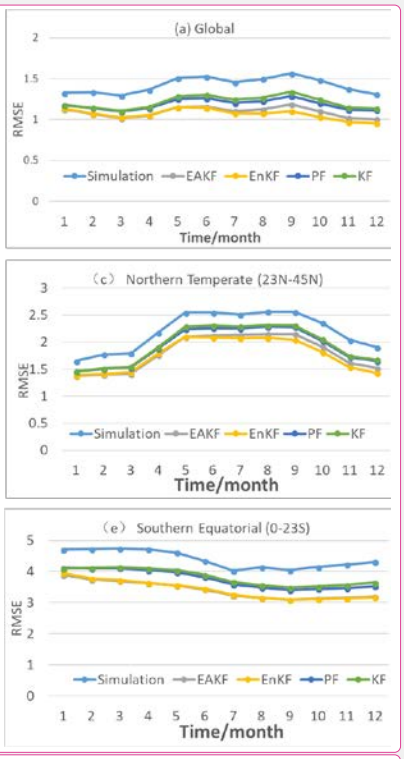

Deleted:

Deleted: RMSEs

Deleted: RMSEs

Deleted: .

Deleted: RMSEs

Deleted: RMSEs

Deleted: lowest RMSE appears for

Deleted: assimilation result with the EAKF method

in other regions, indicating that the assimilation is more efficient there.

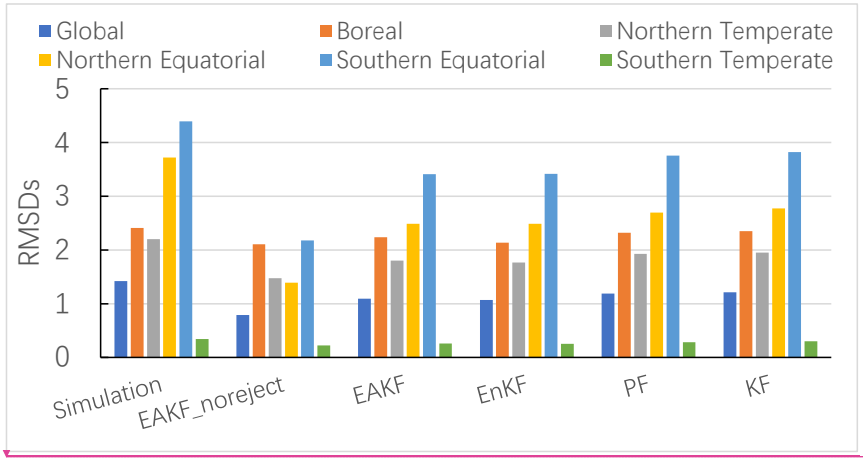

Figure 5: Globally or regionally averaged RMSDs for the simulation/assimilation results.

The background/analysis departures are calculated as (1) innovations, which are the differences between the assimilated LAI and model background, and (2) residuals, which are the differences between the assimilated observations and analysis (Barbu et al., 2011). It was concluded that the LDAS system is working well based on the condition that the residuals are reduced compared to the innovations (Albergel et al., 2017). Figure 6 shows the histograms of innovation and residuals of LAI globally and for all subregions during July 2002. Generally, the distribution characteristics of both innovations and residuals are similar for the algorithms of KF and PF, which means that these two algorithms are not very efficient for LAI assimilation. The distribution of residuals is more centered on 0 than that of the innovations for the EAKF and EnKF algorithms, especially for the EAKF algorithm. The innovations dominantly exhibit a large negative bias, indicating that the model always highly overestimates LAI. The residuals can improve this overestimation situation, especially for the EAKF algorithm. The analysis departures show an abnormal high value in the range of -3 to -2 for the boreal and southern equatorial subregions for the EnKF algorithm but not for the EAKF algorithm, implying that the EAKF algorithm is the optimal algorithm for LAI assimilation.

Deleted: EAKF is the best algorithm

Deleted:

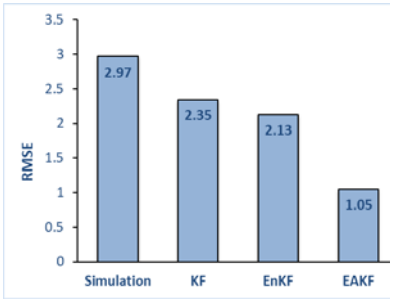

Deleted: RMSEs

Deleted: observations

Deleted: identical

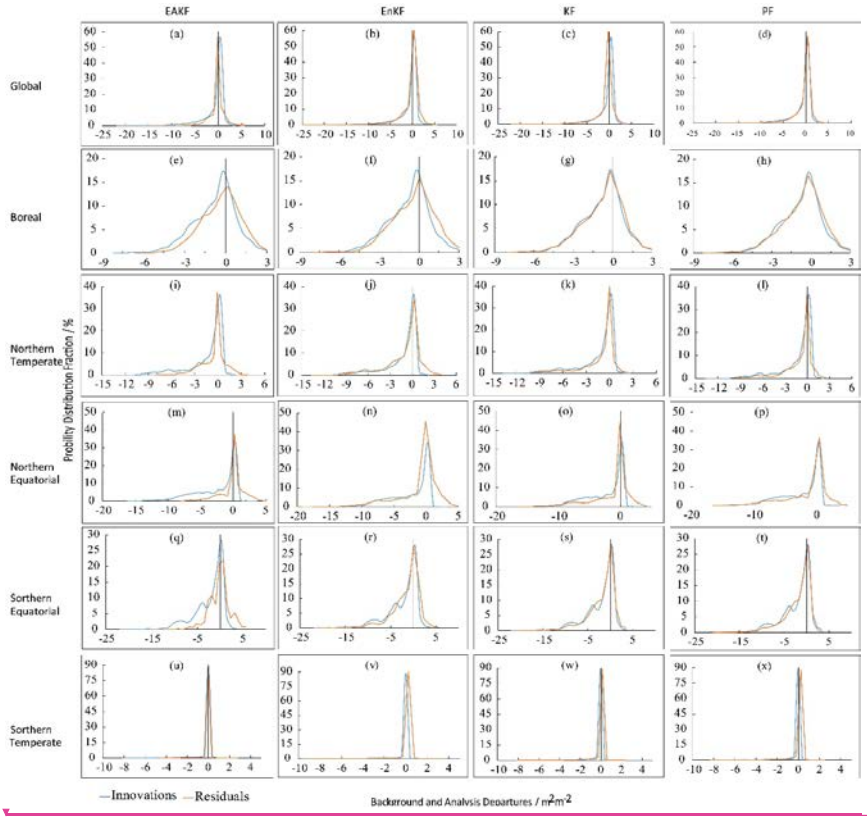

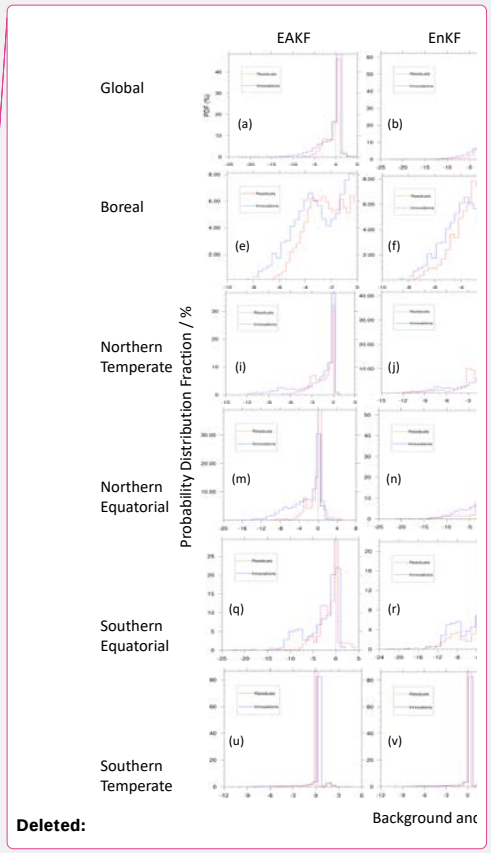

Deleted:

Background and

Figure 6: The histograms of innovation and residuals of LAI globally and for all subregions during July 2002. (a-d) Global; (e-h) boreal; (i-l) northern temperate; (m-p) northern equatorial; (q-t) southern equatorial; (u-x) southern temperate

4 Effective Observational Proportion

The assimilation results depend not only on the algorithm but also on the observations. This not only requires a sufficiently strong degree of discretization for ensemble simulations but also requires the observational variables to be sufficiently trustworthy. In this section, the proportion of LAI observations that can be accepted for the four algorithms is discussed. During assimilation, the DART can calculate the number of non-assimilated observations when the difference of prior mean and observations is larger than three times of the expected value. The proportion of accepted LAI observations is defined as the number of accepted observations divided by the number of total observations.

To explain the relationship between assimilation algorithms and observation rejection, Fig. 7 displays the proportion of accepted LAI observations for the four algorithms in the zonal regions. In general, the EnKF and EAKF methods accepted many more observational LAI observations than the PF and KF methods. In the low-latitude regions, the proportion of accepted LAI observations is

approximately 75%, which is lower than in the high-latitude regions. This may be because the broadleaf forest in tropical regions can grow unrestrictedly in the model, producing LAI values that are much higher than the observations. At the very beginning of assimilation, DART rejects the largest proportion of LAI observations in the southern equatorial, northern equatorial, and northern temperate zones due to large biases between the simulation and the observations. Over time, the rejection proportion gradually decreases for the northern equatorial, southern equatorial and southern temperate. As ensemble-analyzed LAI values tend to relatively fixed, the rejection proportion increases over regions with small LAI amplitudes, such as the northern temperate and boreal region. From May to September in the boreal region and from April to September in the northern temperate region, the proportion of accepted LAI is much smaller than in the other regions. These two periods are also when the model simulation presents an obvious discrete characteristic. This experiment illustrates the utility of the spin-up process for ensemble initial conditions.

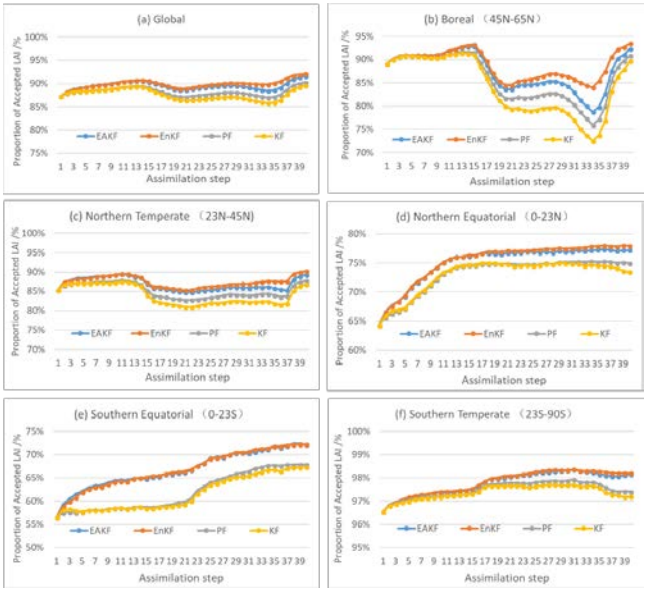

Figure 7: The proportion of accepted LAI observations for the four algorithms in the zonal regions.

The difference between globally assimilated and observed LAIs with the methods of EAKF (with rejection) in (a) July and (b) November are shown in Fig. 8 to illustrate the role of observation proportion. It can be concluded that when accepting all the observations, the assimilation results seem to be better than when some observations are rejected during assimilation. Large biases occur in the Amazon, central Africa, southern Eurasia, and the boreal region, where the LAI is overestimated in the model. Furthermore, the KF and PF algorithms gradually reduce the acceptance of observations as assimilation progresses, which may partially explain their worse performance than the EnKF and EAKF algorithms (see Fig. 5).

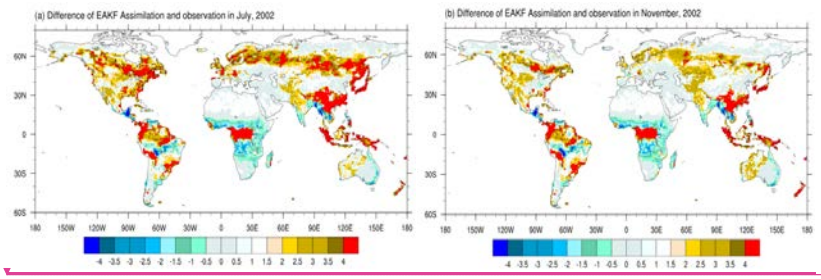

Figure 8: Differences between globally assimilated and observed LAIs for the methods of EAKF in (a) July and (b) November.

During assimilation, the assimilated observations (GLASS LAI) are always treated as "true" values. The question thus becomes how do the true values influence the assimilation results? Figure 9 shows the RMSDs of simulation experiments without/with rejection (EAKF_noreject / EAKF_reject) and MODIS LAI over the (a) global, (b) boreal, (c) northern temperate, (d) northern equatorial, (e) southern equatorial, and (f) southern temperate regions. In the EAKF_reject experimental design, if the observed LAI is three times larger than the bias between the simulation and the observations, the observation would be rejected by DART, while in the EAKF_noreject experiment, all observed LAIs are assimilated. Generally, RMSDs for both simulation and assimilation present obvious annual variations, with RMSDs reaching their maximum values in the season with considerable vegetation growth over a large area. The RMSD of assimilation is far less than that of the simulation, although their characteristic variation patterns are similar. This demonstrates the effectiveness of assimilation for improving model simulation. The RMSD relative to the observations was highest for the simulation, followed by the EAKF_reject experiment, and was lowest for the EAKF_noreject experiment. The RMSDs are large during the growing season, when LAI values are also high in the boreal and northern temperate regions. During assimilation, when accepting all the observations, the RMSD is smaller than that when rejecting some observations.

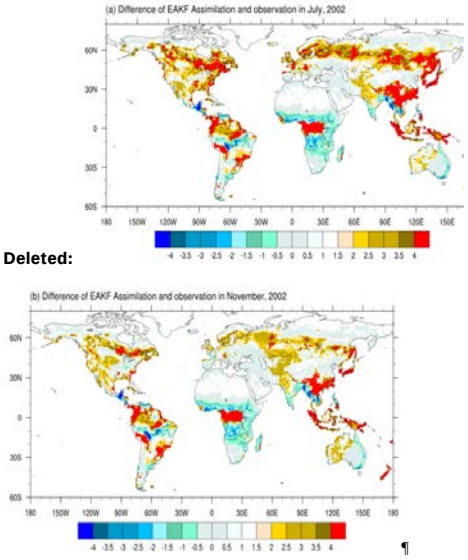

Deleted: RMSEs

Deleted: RMSEs

Deleted: RMSEs

Deleted: RMSE

Deleted: RMSE

Deleted: RMSEs

Deleted: RMSE

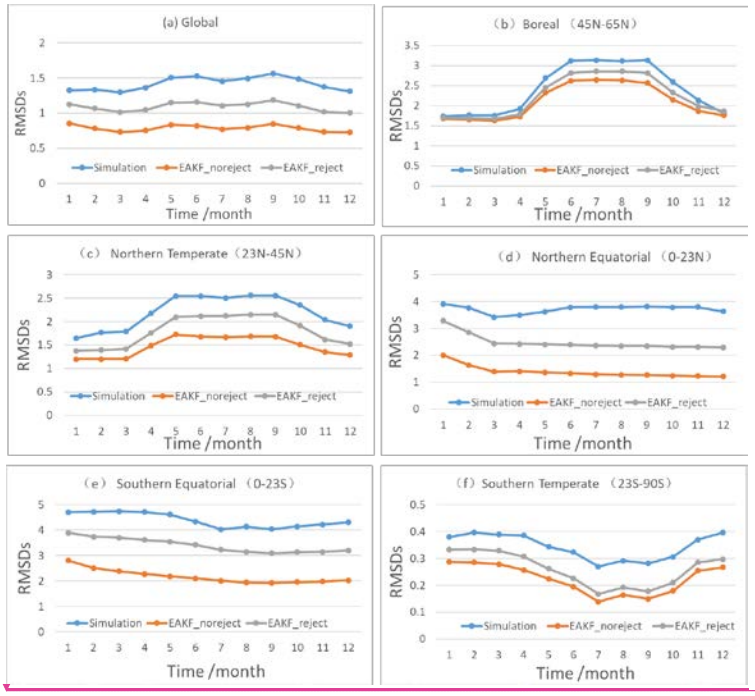

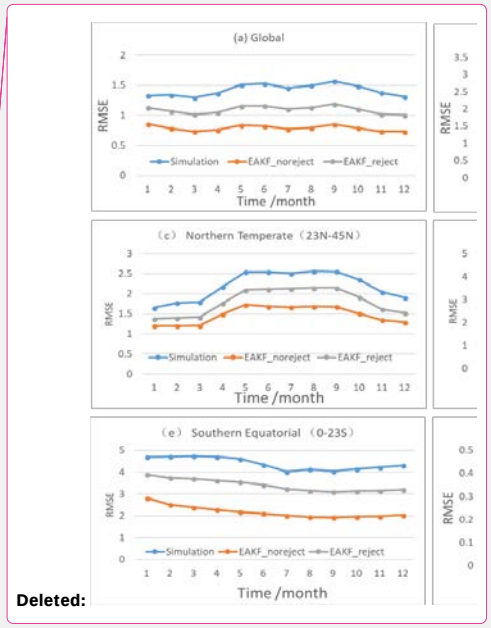

Deleted:

Figure 9: RMSDs of simulation experiments without/with rejection (EAKF_noreject and EAKF_reject) and MODIS LAI for the (a) globe, (b) boreal (45-65°N), (c) northern temperate (23-45°N), (d) northern equatorial (0-23°N), (e) southern equatorial (0-23°S), and (f) southern temperate (23-90°S) regions.

Deleted: RMSEs

Deleted: global

5 Conclusions and Discussion

The Community Land Model version 4 with prognostic carbon-nitrogen components (CLM4CN) is coupled with the Data Assimilation Research Testbed (DART) to determine the optimal assimilation algorithm for leaf area index (LAI). Four different sequential methods, i.e., the Kalman Filter (KF), Ensemble Kalman Filter (EnKF), Ensemble Adjust Kalman Filter (EAKF), and Particle Filter (PF), are discussed in this paper.

The results show that assimilating remotely sensed LAI into the CLM4CN is an effective method for improving model performance. Globally speaking, the EAKF and EnKF assimilation algorithms are better than the KF and PF assimilation algorithms. The LAI obtained by the EAKF method is more continuous than that obtained by the EnKF method and more consistent with observations in central South American and central Africa, whereas the deviation in the EnKF method can be from -4 m^2 m^{-2} to 4 m^2 m^{-2}. Furthermore, the assimilation shows better performance in the vegetation growing season. The

lowest root mean square error (RMSD) is associated with the EAKF algorithm, suggesting that the EAKF algorithm is the best and has a robust performance.

The proportion of observations accepted by the model is another topic of this research. The proportion of accepted LAI observations is 10-20% in the low latitudes lower than in the high latitudes because of large biases between the assimilation and the observations. When all the observations are accepted, the RMSD of the results is smaller than that when some observations are rejected.

Deleted: RMSE

Deleted: RMSE

Code availability. The Community Land Model version 4.0 with carbon and nitrogen Components (CLM4CN) is a part of the Community Earth System Model version 1.1.1 (CESM1.1.1) developed by the National Center for Atmospheric Research (NCAR). The CESM code can be downloaded from http://www.cesm.ucar.edu/index.html. Developed and maintained by the Data Assimilation Research Section (DAReS) at NCAR, Data Assimilation Research Testbed (DART version lanai) can be downloaded from https://www.image.ucar.edu/DAReS/DART/.

Author contributions. All of the authors participated in the development of the paper's findings and recommendations.

Competing interests. The authors declare that they have no conflict of interest.

Acknowledgments. This work was jointly supported in part by the National Natural Science Foundation of China (2016YFA0600303 and 2017YFA0604304) and the Jiangsu Collaborative Innovation Center for Climate Change. Kevin Raeder (raeder@ucar.edu) is thanked for providing the DART/CAM4 reanalysis as ensemble meteorological forcing. Tim Hoar, Long Zhao and Yongfei Zhang are thanked for part of the coding and coupling with DART/CLM4CN.

References

Albergel, C., Munier, S., Leroux, D. J., Dewaele, H., Fairbairn, D., Barbu, A. L., Gelati, E., Dorigo, W., Faroux, S., Meurey, C., Moigne, P. L., Decharme, B., Mahfouf, J. F., and Calvet, J. C.: Sequential assimilation of satellite-derived vegetation and soil moisture products using SURFEX_v8.0: LDAS-Monde assessment over the Euro-Mediterranean area, Geosci. Model Develop., 10, 3889-3912, https://doi.org/10.5194/gmd-10-3889-2017, 2017.

Anderson, J. L.: An ensemble adjustment Kalman filter for data assimilation, Mon. Wea. Rev., 129, 2884-2903, 2001.

Anderson, J. L.: A local least squares framework for ensemble filtering, Mon. Wea. Rev., 131, 634-642, 2003.

Anderson, J. L.: An adaptive covariance inflation error correction algorithm for ensemble filters, Tellus, 59(2), 210-224, http://doi.org/10.1111/j.1600-0870.2006.00216.x, 2007.

Anderson, J. L., Hoar, T., Raeder, K., Liu, H., Collins, N., Torn, R. and Arellano, A.: The data assimilation research testbed: A community facility, Bull. Am. Meteorol. Soc., 90(9), 1283-1296, https://doi.org/10.1175/2009BAMS2618.1, 2009.

Deleted:

Bannister, R. N.: A review of operational methods of variational and ensemble variational data assimilation, Q. J. R. Meteorol. Soc., 143, 607-633, 2016.

Barbu, A. L., Calvet, J.-C., Mahfouf, J.-F., Albergel, C., and Lafont, S.: Assimilation of Soil Wetness Index and Leaf Area Index into the ISBA-A-gs land surface model : grassland case study, Biogeosciences, 8, 1971-1986, https://doi.org/10.5194/bg-8-1971-2011, 2011.

Baret, F., Weiss, M., Lacaze, R., Camacho, F., Makhmara, H., Pacholcyzk, P., & Smets, B.: GEOVE: LAI and FAPAR essential climate variables and FCOVER global time series capitalizing over existing products. Part1: Principles of development and production, Remote Sensing of Environment, 137,299-309. doi: 10.1016/j.rse.2012.12.027, 2013.

Bonan, G. B.: Land atmospheric interactions for climate system models: Coupling biophysical, biogeochemical and ecosystem dynamical processes, Remote Sens. Environ., 51, 57-73, 1995.

Bonan, G.B., Pollard, D., Thompson, S.L.: Effects of boreal forest vegetation on global climate, Nature, 359, 716-718, http://doi.org/10.1038/359716a0, 1992.

Burgers, G., van Leeuwen, P. J. and Evensen, G.: Analysis scheme in the ensemble Kalman filter, Mon. Wea. Rev., 126, 1719-1724, 1998.

Carrera, M. L., Belair, S., and Bilodeau, B.: The Canadian Land Data Assimilation System (CaLDAS): Description and Synthetic Evaluation Study, J. Hydrometeo., 16, 1293-1314, http://doi.org/10.1175/JHM-D-14-0089.1, 2015.

Dai, Y. J., Zeng, X. B., and Dickinson, R. E.: The common land model (CLM), Bull. Amer. Meteor. Soc., 84, 1013-1023, http://doi.org/10.1175/BAMS-84-8-1013, 2003.

Danabasoglu, G., Bates, S., Briegleb, B. P., Jayne, S. R., Jochum, M., Large, W. G., Peacock, S., and Yeager, S. G.: The CCSM4 Ocean Component, J. Clim., 25, 1361-1389, http://doi.org/10.1175/JCLI-D-11-00091.1, 2012.

De Lannoy, G. J. M., de Rosnay, P. and Reichle, R. H.: Soil moisture data assimilation. In Handbook of Hydrometeorological Ensemble Forecasting, edited by Q. Duan, F. Pappenberger, J. Thielen, A.Wood, H. Cloke and J. C. Schaake. 2016.

Dimet F. X. L., and Talagrand, O.: Variational algorithms for analysis and assimilation of meteorological observations: theoretical aspects, Tellus, 38A, 97-110, https://doi.org/10.3402/tellusa.v38i2.11706, 1986.

Doucet, A., Godsill, S., and Andrieu, C.: On sequential Monte Carlo sampling methods for Bayesian filtering, Stat. Comput., 10, 197-208, 2000.

Evensen, G.: Sequential data assimilation with a nonlinear quasi-geostrophic model using monte-carlo methods to forecast error statistics, J. Geophys. Res. Oceans, 99(C5), 10143-10162, 1994.

Evensen, G.: The Ensemble Kalman Filter: Theoretical Formulation and Practical Implementation, Ocean Dyn., 53, 343-367, http://doi.org/10.1007/s10236-003-0036-9, 2003.

Evensen, G.: Data Assimilation, the Ensemble Kalman Filter, Springer, pp 279, 2007.

Fertig, E. J., Harlim, J., and Hunt, B. R.: A comparative study of 4D-VAR and a 4D ensemble filter: Perfect model simulations with Lorenz-96, Tellus, 59A, 96-100, http://doi.org/10.1111/j.1600-0870.2006.00205.x, 2007.

Fox, A. M., Hoar, T. J., Anderson, J. L., Arellano, A. F., Smith, W. K., Litvak, M. E., et al.: Evaluation of a data assimilation system for land surface models using CLM4.5. Journal of Advances in Modeling Earth Systems, 10, 2471-2494, 2018.

Gordon, N. J., Salmond, D. J. and Smith, A. F.: Novel approach to nonlinear/non- Gaussian Bayesian state estimation, IEE Proc., 140, 107-113, 1993.

Han, X. J., and Li, X.: An evaluation of the nonlinear/non-Gaussian filters for the sequential data assimilation, Remote Sens. Environ., 112(4), 1434-1449, http://doi.org/10.1016/j.rse.2007.07.008, 2008.

Houtekamer, P. L., and Mitchell, H.: Data assimilation using an ensemble Kalman filter technique, Mon. Wea. Rev., 126(3), 796-811, 1998.

Houtekamer, P. L., Mitchell, H. L., Pellerin, G., Buehner, M., Charron, M., Spacek, L., and Hansen, B.: Atmospheric data assimilation with an ensemble Kalman filter: Results with real observations, Mon. Wea. Rev., 133, 604-620, 2005.

Huang, C. L., and Li, X.: A Review of Land Data Assimilation System, Remote Sens. Techn. Appl., 19, 424-024.

Hunt, B. R., Kalnay, E., Kostelich, E. J., Ott, E., Patil, D. J., and Sauer, T.: Four-dimensional ensemble Kalman filtering, Tellus, 56A, 273-277, 2004.

Hu, S. J., Qiu, C. Y., Zhang, L. Y., Huang, Q. C., Yu, H. P., and Chou, J. F.: An approach to estimating and extrapolating model error based on inverse problem methods: towards accurate numerical weather prediction, Chin. Phys. B, 23, 089201, http://doi.org/10.1088/1674-1056/23/8/089201, 2014.

Ines, A. V. M., Das, N. N., Hansen, J. P. and Njoku, E. G.: Assimilation of remotely sensed soil moisture and vegetation with a crop simulation model for maize yield prediction, Remote Sensing of Environment, 138, 149-164, 2013.

Jacobs, C. M. J., Moors, E. J., Maat, H. W. Ter., Teuling, A. J., Balsamo, G., Bergaoui, K., Ettema, J., Lange, M., Hurk, B. J. J. M. Van Den, Viterbo, P., and Wergen, W.: Evaluation of European Land Data Assimilation System (ELDAS) products using in situ observations, Tellus, 60A, 1023-1037, http://doi.org/10.1111/j.1600-0870.2008.00351.x, 2008.

Jin, X., Kumar, L., Li, Z., Xu, X., Yang, G. and Wang, J.: A review of data assimilation of remote sensing and crop models, Eur. J. Agron., 92, 141-152, 2018.

Kalman, R. E.: A new approach to linear filtering and prediction problems. Trans. ASME J. Basic Eng., 82(D), 35-45, 1960.

Kalnay, E.: Amospheric Modeling, Data Assimilation and Predictability, Cambridge University Press, pp 512, 2003.

Kalnay, E., Li, H., Miyoshi, T., Yang, S. -C., and Ballabrera-Poy, J.: 4-D-Var or ensemble Kalman filter?, Tellus, 59A, 758-773, http://doi.org/10.1111/j.1600-0870.2007.00261.x, 2007.

Knyazikhin, Y., Martonchik, J. V., Myneni, R. B., Diner, D. J., and Running, S. W.: Synergistic algorithm for estimating vegetation canopy leaf area index and fraction of absorbed photosynthetically active radiation from MODIS and MISR data, J. Geophys. Res., 103, 32257-32275, 1998.

Kwon, Y., Yang, Z. L., Zhao, L., Hoar, T. J., Toure, A. M., and Rodell, M.: Estimating snow water storage in North America using CLM4, DART, and Snow Radiance Data Assimilation, J. Hydrometeo., 17, 2853-2874, http://doi.org/10.1175/JHM-D-16-0028.1, 2016.

Lahoz, W. A. and De Lannoy, G. J. M.: Closing the Gaps in Our Knowledge of the Hydrological Cycle over Land: Conceptual Problems, Surv. Geophys., 35, 623-660, 2014.

Lawrence, P. J., and Chase, T. N.: Representing a new MODIS consistent land surface in the Community Land Model (CLM 3.0), J. Geophys. Res., 112, G01023, http://doi.org/10.1029/2006JG000168, 2007.

Leng, H. Z., and Song, J. Q.: Hybrid three-dimensional variation and particle filtering for nonlinear systems, Chin. Phys. B, 22, 030505, http://doi.org/10.1088/1674-1056/22/3/030505, 2013.

Levis, S., Bonan, G. B., Vertenstein, M., and Oleson, K. W.: The Community Land Model's Dynamic Global Vegetation Model (CLM-DGVM): Technical Description and User's Guide, Boulder, Colorado: National Center for Atmospheric Research, NCAR/TN-459+IA, 2004.

Lindgren, F, Geladi, P, Wold, S.: The kernel algorithm for PLS, J. Chemometrics, 7, 45, 1993.

Liu，Q., L. Gu, R. E. Dickinson, et al.: Assimilation of satellite reflectance data into a dynamical leaf model to infer seasonally varying leaf areas for climate and carbon models, J. Geophy. Res., 113, D19113, doi: 10.1029/2007JD009645, 2008.

Li, X. J., Xiao, Z. Q., Wang, J. D., Qu, Y., and Jin, H. A.: Dual Ensemble Kalman Filter assimilation method for estimating time series LAI, J. Remote. Sens., 18, 27-44, http://doi.org/10.11834/jrs.20133036, 2014.

Li, Y., Zhao, M. S., Motesharrei, S., Mu, Q. Z., Kalnay, E., and Li, S. C.: Local cooling and warming effects of forests based on satellite observations, Nat. Commun., 6, 6603, http://doi.org/10.1038/ncomms7603, 2015.

Lin, P. R., Wei, J. F., Yang, Z. L., Zhang, Y. F., and Zhang, K.: Snow data assimilation-constrained land initialization improves seasonal temperature prediction, Geophy. Res. Lett., 43, 11423, http://doi.org/10.1002/2016GL070966, 2016.

Luo, L. F., Robock, A., Mitchell, K. E., Houser, P. R., Wood, E. F., Schaake, J. C., Lohmann, D., Cosgrove, B., Wen, F. H., Sheffield, J., Duan, Q. Y., Higgins, R. W., Pinker, R. T., and Tarpldy, D.: Validation of the North American Land Data Assimilation System (NLDAS) retrospective forcing over the southern Great Plains, J. Geophys. Res. Atmos., 108, 8843, http://doi.org/10.1029/2002JD003246, 2003.

Mitchell, K. E., Lohmann, D., Houser, P. R., Wood, E. F., Schaake, J. C., Robock, A., Cosgrove, B. A., Sheffield, J., Duan, Q. Y., Luo, L. F., Higgins, R. W., Pinker, R. T., Tarpley, J. D., Lettenmaier, D. P., Marchall, C. H., Entin, J. K., Pan, M. Koren, V., Meng, J., Ramsay, B. H., and Bailey, A. A.: The multi-institution North American Land Data Assimilation System (NLDAS): Utilizing multiple GCIP products and partners in a continental distributed hydrological modeling system, J. Geophys. Res., 109, D07S90, http://doi.org/10.1029/2003JD003823, 2004.

Mokhtari, A., Noory, H. and Vazifedoust, M. : Improving crop yield estimation by assimilating LAI and inputting satellitebased surface incoming solar radiation into SWAP model, Agr. Forest Meteorol., 250-251, 159-170, https://doi.org/10.1016/j.agrformet.2017.12.250, 2018.

Montzka, C., Pauwels, V. R. N., Franssen, H.-J. H., Han, X.-J., and Vereecken, H.: Multivariate and multiscale data assimilation in terrestrial systems: a review, Sensors, 12, 16291-16333, https://doi.org/10.3390/s121216291, 2012.

Moradkhani, H., Hsu, K. L., Gupta, H., Sorooshian, S.: Uncertainty assessment of hydrologic model states and parameters: Sequential data assimilation using the particle filter, Water Resour. Res., 41(5), W05012, http://doi.org/10.1029/2004WR003604, 2005.

Oleson, K. W., Lawrence, D. M., Bonan, G. B., Flanner, M. G., Kluzek, E., Lawrence, P. J., Levis, S., Swenson, S. C., Thornton, P. E., Dai, A. G., Decker, M., Dickinson, R., Feddema, J., Heald, C. L., Hoffman, F., Lamarque, J. -F., Mahowald, N., Niu, G. Y., Qian, T. T., Randerson, J., Running, S., Sakaguchi, K., Slater, A., Stöckli, R., Wang, A. H., Yang, Z. L., Zeng, X. D., and Zeng, X. B.: Technical Description of Version 4.0 of the Community Land Model, NCAR Tech Note (NCAR/TN-478 + STR) 257pp, 2010.

Pitman, A. J.: The evolution of, and revolution in, land surface schemes designed for climate models, Int. J. Climatol., 23(5), 479-510, http://doi.org/10.1002/joc.893, 2003.

Pitman, A. J., Noblet-Ducoudré, N. de, Cruz, F. T., Davin, E. L., Bonan, G. B., Brovkin, V., Claussen, M., Delire, C., Ganzeveld, L., Gayler, V., van den Hurk, B.J.J.M., Lawrence, P. J., van der Molen, M. K., Müller, C., Reick, C. H., Seneviratne, S. I., Strengers, B. J., and Voldoire, A.: Uncertainties in climate responses to past land cover change: First results from the LUCID intercomparison study, Geophys. Res. Lett., 36, L14814, http://doi.org/10.1029/2009GL039076, 2009.

Qian, T. T., Dai, A. G., Trenberth, K. E., & Oleson, K.W.: Simulation of global land surface conditions from 1948 to 2004: Part I: Forcing data and evaluations, J. Hydrometeor., 7(5), 953-975, doi:10.1175/JHM540.1, 2006.

Raeder, K., Anderson, J. L., Collins, N., Hoar, T. J., Kay, J. E., Lauritzen, P. H., and Pincus, R., DART/CAM: An Ensemble Data Assimilation System for CESM Atmospheric Models, J. Clim., 25, 6304-6317, http://doi.org/10.1175/JCLI-D-11-00395.1, 2012.

Reichle, R. H., De Lannoy, G. J. M., Forman, B. A., Draper, C. S. and Liu, Q.: Connecting Satellite Observations with Water Cycle Variables Through Land Data Assimilation: Examples Using the NASA GEOS-5 LDAS, Surv. Geophys., 35, 577-606, 2014.

Rodell, M., Houser, P. R., Jambor, U., Gottschalck, J., Mitchell, K., Meng, C. J., Arsenault, K., Cosgrove, B., Radakovich, J., Bosilovich, M., Entin, J. K., Walker, J. P., Lohmann, D., and Toll, D.: The global land data assimilation system, Bull. Amer. Meteor. Soc., 85, 381-394, http://doi.org/10.1175/BAMS-85-3-381, 2004.

Sabater, J. M., Rüdiger, C., Calvet, J.-C., Fritz, N., Jarlan, L. and Kerr Y.: Joint assimilation of surface soil moisture and LAI observations into a land surface model, Agr. Forest Meteorol., 148, 1362-1373, 2008.

Sawada, Y., Koike, T. and Walker, J. P.: A land data assimilation system for simultaneous simulation of soil moisture and vegetation dynamics. J. Geophys. Res. Atmos., 120, 5910-5930, 2015.

Sawada, Y.: Quantifying Drought Propagation from Soil Moisture to Vegetation Dynamics Using a Newly Developed Ecohydrological Land Reanalysis, Remote Sens., 10, 1197, 2018.

Deleted: .

Shi, M.J., Yang, Z. L., Lawrence, D. M., Dickinson, R. E., & Subin, Z. M.: Spin-up processes in the Community Land Model version 4 with explicit carbon and nitrogen components. Ecological Modelling, 263, 308-325, doi:10.1016/j.ecolmodel.2013.04.008, 2013.

Thornton, P. E., and Zimmermann, N.E.: An improved canopy integration scheme for a land surface model with prognostic canopy structure, J. Clim., 20, 3092-3923, http://doi.org/10.1175/JCLI4222.1, 2007.

Vetra-Carvalho, S., van Leeuwen, P. J., Nerger, L., Barth, A., Altaf, M. U., Brasseur, P. Kirchgessner, P. and Beckers, J.-M.: State-of-the-art stochastic data assimilation methods for high-dimensional non-Gaussian problems, Tellus A, 70, 1445364, 2018.

Viskari, T., Hardiman, B., Deasi, A. R., and Dietz, M. C.: Model-data assimilation of multiple phenological observations to constrain and predict leaf area index, Ecol. Appl., 25, 546-558, 2015.

Wan, L. Y., Zhu, J., Wang, H., Yan, C. X., and Bertino, L.: A "dressed" ensemble Kalman filter using the hybrid coordinate ocean model in the pacific, Adv. Atmos. Sci., 26(5). 1042-1052, http://doi.org/10.1007/s00376-009-7208-6, 2009.

Wang, X. G., Hamill, T. M., Whitaker, J. S., and Bishop, C. H.: A Comparison of Hybrid Ensemble Transform Kalman Filter-Optimum Interpolation and Ensemble Square Root Filter Analysis Schemes, Mon. Wea. Rev., 135, 1055-1076, http://doi.org/10.1175/MWR3307.1, 2007.

Whitaker, J. S., and Hamill, T. M.: Ensemble data assimilation without perturbed observations, Mon. Wea. Rev., 130, 1913-1924, 2002.

Whitaker, J. S., Hamill, T. M., Wei, X., Song, Y., and Toth, Z.: Ensemble data assimilation with the NCEP global forecasting system, Mon. Wea. Rev., 136, 463-482, http://doi.org/10.1175/2007MWR2018.1, 2008.

Wu, X. R., Han, G. J., Li, D., and Li, W.: A hybrid ensemble filter and 3D variational analysis scheme, J. Trop. Oceanogr. (in Chinese), 30(6), 24-30, 2011.

Xia, Y. L., Mitchell, K., Ek, M., Cosgrove, B., Sheffield, J., Luo, L. F., Alonge, C., Wei, H., Meng, J., Livneh, B., Duan, Q. Y., and Lohmann, D.: Continental-scale water and energy flux analysis and validation for North American Land Data Assimilation System project phase 2 (NLDAS-2): 2. Validation of model-simulated streamflow, J. Geophys. Res., 117, D03109, http://doi.org/10.1029/2011JD016051, 2012.

Xiao, Z. Q., Liang, S. L., Wang, J. D., and Wu, X. Y.: Use of an ensemble Kalman Filter for real-time inversion of Leaf Area Index from MODIS time series data, IEEE Trans. Geosci. Remote Sens., 4: 73-76, 2009.

Yuan, H., Dai, Y. J., Xiao, Z. Q., Ji, D. Y., & Wei, S. G.: Reprocessing the MODIS Leaf Area Index products for land surface and climate modelling. Remote Sensing of Environment, 115, 1171-1187. doi: 10.1016/j.rse.2011.01.001, 2011.

Zhang, F. Q., Zhang, M., and Hansen, J. A.: Coupling Ensemble Kalman Filter with Four-dimensional Variational Data Assimilation, Adv. Atmos. Sci., 26, 1-8, http://doi.org/10.1007/s00376-009-0001-8, 2009.

Zhang, L., Huang, S. X., Shen, C., and Shi, W. L.: Variational assimilation in combination with the regularization method for sea level pressure retrieval from QuickSCAT scatterometer data I:

Theoretical frame construction, Chin. Phys. B, 20(11), 119201, http://doi.org/10.1088/1674-1056/20/11/119201, 2011.

Zhang, Y. F., Hoar, T. J., Yang, Z. L., Anderson, J. L., Toure, A. M., and Rodell, M.: Assimilation of MODIS snow cover through the Data Assimilation Research Testbed and the Community Land Model version 4, J. Geophys. Res. Atmos., 119, 7091-7103, http://doi.org/10.1002/2013JD021329, 2014.

Zhao, L., Yang, Z. L., Hoar, T. J.: Global Soil Moisture Estimation by Assimilating AMSR-E Brightness Temperatures in a Coupled CLM4-RTM-DART System, J. Hydrometeo., 17, 2431-2454, http://doi.org/10.1175/JHM-D-15-0218.1, 2016.

Zhao, L., and Yang, Z. L.: Multi-sensor land data assimilation: Toward a robust global soil moisture and snow estimation, Remote Sens. Environ., 216, 13-27, https://doi.org/10.1016/j.rse.2018.06.033, 2018.

Zhao, X., Liang, S. L., Liu, S. H., Yuan, W. P., Xiao, Z. Q., Liu, Q., et al.: The Global Land Surface Satellite (GLASS) Remote Sensing Data Processing System and Products. Remote Sensing, 5, 2436-2450. doi:10.3390/rs5052436, 2013.

Zupanski, M.: Maximum likelihood ensemble filter: Theoretical aspects, Mon. Wea. Rev., 133, 1710-1726, 2005.